

CONFIDENTIAL

Copy 326
RM L53G13

NACA RM L53G13



RESEARCH MEMORANDUM

INVESTIGATION OF THE EFFECTS OF LEADING-EDGE FLAPS ON
THE AERODYNAMIC CHARACTERISTICS IN PITCH AT MACH
NUMBERS FROM 0.40 TO 0.93 OF A WING-FUSELAGE
CONFIGURATION WITH A 45° SWEPTBACK WING
OF ASPECT RATIO 4

By Kenneth P. Spreemann and William J. Alford, Jr.

Langley Aeronautical Laboratory
Langley Field, Va.

CLASSIFIED DOCUMENT

This material contains information affecting the National Defense of the United States within the meaning of the espionage laws, Title 18, U.S.C., Secs. 793 and 794, the transmission or revelation of which in any manner to an unauthorized person is prohibited by law.

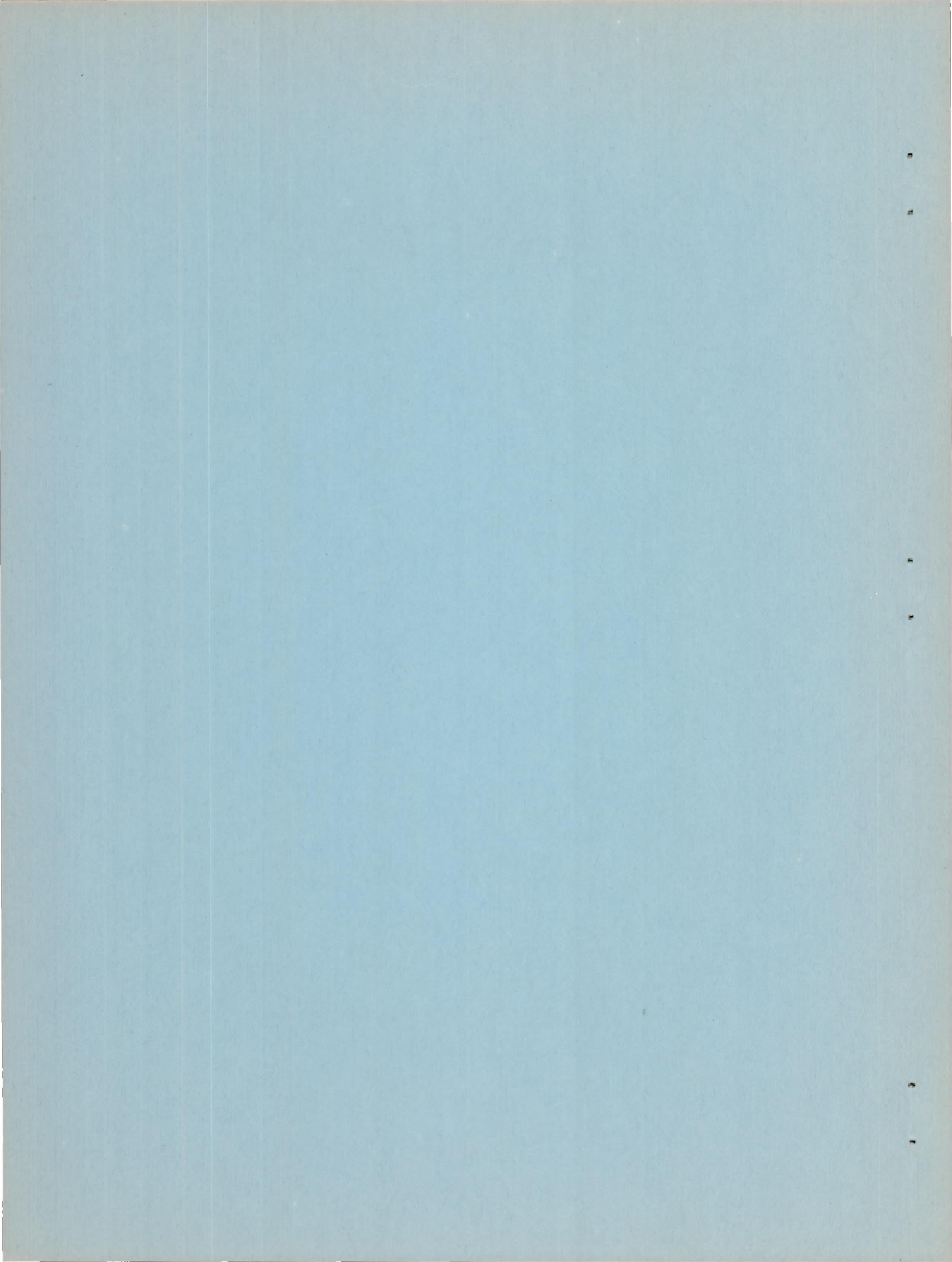
CLASSIFICATION CHANGED TO UNCLASSIFIED
AUTHORITY: NACA RESEARCH ABSTRACT NO. 104
DATE: AUGUST 3, 1956

WHI

NATIONAL ADVISORY COMMITTEE FOR AERONAUTICS

WASHINGTON
August 20, 1953

CONFIDENTIAL



NATIONAL ADVISORY COMMITTEE FOR AERONAUTICS

RESEARCH MEMORANDUM

INVESTIGATION OF THE EFFECTS OF LEADING-EDGE FLAPS ON
THE AERODYNAMIC CHARACTERISTICS IN PITCH AT MACH
NUMBERS FROM 0.40 TO 0.93 OF A WING-FUSELAGE
CONFIGURATION WITH A 45° SWEEPBACK WING
OF ASPECT RATIO 4

By Kenneth P. Spreemann and William J. Alford, Jr.

SUMMARY

An investigation was made to determine the effects of a number of leading-edge flaps on the aerodynamic characteristics in pitch of a wing-fuselage configuration with a 45° sweptback wing of aspect ratio 4, taper ratio 0.3, and NACA 65A006 airfoil section. The investigation was made in the Langley high-speed 7- by 10-foot tunnel over a Mach number range of 0.40 to 0.93 and an angle-of-attack range of about -2° to 24°. Lift, drag, and pitching-moment data were obtained for all configurations.

All the leading-edge flaps investigated reduced the drag in the medium lift range. Full-span and outboard partial-span flaps deflected 3° or 6° usually gave better maximum lift-drag ratios than any of the other leading-edge flap arrangements investigated throughout the Mach number range. In general, all leading-edge flaps delayed the sharp pitch-up tendencies of this model by from 0.2 to 0.4 lift coefficient up to a Mach number of 0.90, but provided little or no improvement at the highest Mach numbers investigated.

INTRODUCTION

Previous investigations at high subsonic speeds have shown that the lift-drag ratios of low-aspect-ratio sweptback wings could be substantially improved with low-angle leading-edge flap deflections up to a Mach number of 0.90 (refs. 1 and 2). As a result of these investigations study of a more comprehensive range of full-span and partial-span deflections

was considered desirable in order to determine whether additional improvements could be obtained in the lift-drag ratios throughout the subsonic Mach number range. The purpose of the present investigation was, therefore, to determine the effects of full-span and various partial-span combinations of leading-edge flaps on the aerodynamic characteristics in pitch of a 45° sweptback wing of aspect ratio 4, taper ratio 0.3, and NACA 65A006 airfoil section.

A preliminary study of the data in this paper indicated that the 6° full-span and the 3° outboard partial-span leading-edge flaps were, in general, the best leading-edge flap arrangements for improving the maximum lift-drag ratios of this model. Data for these two configurations and for the basic wing-fuselage configuration were presented in reference 3 as a basis of comparison in an investigation of the use of chord extensions or fences in combination with these flap arrangements as a means of improving simultaneously the high-lift stability and the lift-drag ratios.

The present investigation was made in the Langley high-speed 7- by 10-foot tunnel over a Mach number range of 0.40 to 0.93 and an angle-of-attack range of about -2° to 24° . Lift, drag, and pitching moments were obtained for all configurations.

COEFFICIENTS AND SYMBOLS

The coefficients and symbols used in this paper are defined as follows:

C_L	lift coefficient, $Lift/qS$
C_D	drag coefficient, $Drag/qS$
C_m	pitching-moment coefficient referred to $0.25\bar{c}$, $\frac{\text{Pitching moment}}{qS\bar{c}}$
C_{D_b}	base-pressure drag coefficient
q	dynamic pressure, $\frac{1}{2}\rho V^2$, lb/sq ft
S	wing area, sq ft (2.25 on model)
S_b	area of base of model, sq ft (0.059 on model)

\bar{c}	mean aerodynamic chord of wing, $\frac{2}{S} \int_0^{b/2} c^2 dy$, ft
c	local wing chord, parallel to plane of symmetry, ft
b	wing span, ft
ρ	air density, slugs/cu ft
V	free-stream velocity, ft/sec
P_0	free-stream static pressure, lb/sq ft
P_b	static pressure at base of model, lb/sq ft
M	Mach number
R	Reynolds number of wing based on \bar{c}
α	angle of attack of fuselage center line, deg
$\Delta\alpha$	change in local angle of attack due to distortion of wing, deg
K	correction factor for $C_{L\alpha}$ due to wing distortion
$C_{L\alpha}$	lift-curve slope, $\frac{\partial C_L}{\partial \alpha}$
$\Delta \left(\frac{\partial C_m}{\partial C_L} \right)$	incremental change in aerodynamic-center location due to wing distortion
y	spanwise distance from plane of symmetry, ft
δ_n	leading-edge flap deflection angle, deg (see fig. 1)
A	leading-edge flap that extends from 0.139 $b/2$ to 0.426 $b/2$
B	leading-edge flap that extends from 0.426 $b/2$ to 0.713 $b/2$
C	leading-edge flap that extends from 0.713 $b/2$ to 1.00 $b/2$

MODEL AND APPARATUS

A drawing of the wing-fuselage combination showing details of the leading-edge flaps employed is presented in figure 1. A photograph of a typical sweptback-wing model mounted on the sting in the Langley high-speed 7- by 10-foot tunnel is shown as figure 2. The wing employed in this investigation had 45° sweepback of the quarter-chord line, aspect ratio 4, taper ratio 0.3, and an NACA 65A006 airfoil section parallel to the plane of symmetry. Ordinates of the fuselage are given in table I.

The leading-edge flap was established by cutting the wing along the 20-percent-chord line, and flap angles were obtained with preset steel inserts. After setting a desired flap angle, the groove in the wing was filled and finished flush to the wing surface. The junctures between flaps were sealed for all tests. The full-span flap deflection angles and the partial-span flap deflection angle combinations employed are listed in table II. Angular distortion of the flap under load was negligible.

The model was tested on the sting-type support system shown in figure 2. With this system the model was remotely operated through an angle-of-attack range of about -2° to 24° . A strain-gage balance mounted inside the fuselage was used to measure the forces and moments of the wing-fuselage combination.

TESTS AND CORRECTIONS

The investigation was made in the Langley high-speed 7- by 10-foot tunnel. Lift, drag, and pitching moment were measured through a Mach number range of 0.40 to 0.93 and an angle-of-attack range of about -2° to 24° . The size of the model caused the tunnel to choke at a corrected Mach number of about 0.95 for the zero-lift condition, although partial-choking conditions may have occurred in the high angle-of-attack range at a Mach number of 0.93.

Blockage corrections were determined by the method of reference 4 and were applied to the Mach numbers and dynamic pressures. Jet-boundary corrections, applied to the angle of attack and drag, were calculated by the method of reference 5. The jet-boundary corrections to pitching moment were considered negligible and were not applied to the data. Corrections to the drag coefficients for buoyancy due to longitudinal pressure gradients varied from about 0.0015 at $M = 0.40$ to about 0.0017 at $M = 0.90$. These corrections were not applied to the data.

No tare corrections were obtained; however, previous experience (ref. 6, for example) indicates that for a tailless sting-mounted model, similar to the model investigated herein, the tare corrections to lift and pitching moment are negligible. The drag data have been corrected to correspond to a pressure at the base of the fuselage equal to free-stream static pressure. For this correction, the base pressure was determined by measuring the pressure inside the fuselage at a point about 9 inches forward of the base. The drag correction (base-pressure drag coefficient C_{D_b}) was calculated from the measured pressure data by the relation

$$C_{D_b} = \frac{P_b - P_o}{q} \frac{S_b}{S}$$

Values of C_{D_b} for average test conditions are presented in figure 3. The corrected model drag data were obtained by adding the base-pressure drag coefficient to the drag coefficient determined from the strain-gage measurements.

The angle of attack has been corrected for deflection of the sting support system under load. Correction factors for the effects of aeroelastic distortion of the wing were obtained by static loading to simulate elliptic span loading and these correction factors are presented in figure 4. These correction factors were not applied to the data.

The mean Reynolds number variation with Mach number for the wing of this investigation is presented in figure 5.

RESULTS AND DISCUSSION

The data are presented in figures 6 to 15; a detailed listing of the data is given in table II. The data for the basic wing-fuselage configuration (no flap deflection) are presented in each figure to provide a basis for comparison. The basic longitudinal aerodynamic data for each configuration are given for a range of Mach numbers from 0.40 to 0.93 in figures 6 to 11. The lift-drag ratios for each configuration are presented for three representative Mach numbers in figures 12-15. In order to expedite the publication of these data only a brief analysis of the data is included herein.

Generally, there were no significantly large effects on the lift characteristics for any of the leading-edge flap arrangements investigated (see parts (a) of figures 6 to 11). In some cases, the leading-edge

flap arrangements produced slightly higher lift-curve slopes than did the basic wing-fuselage combination (configuration 1). Irregular increases in C_L were evidenced in the high angle-of-attack range except at a Mach number of 0.93 at which the tunnel power limitations precluded securing the higher angle-of-attack range.

In most cases, especially the 10° and 15° partial-span leading-edge flap deflections (fig. 9(c), configurations 8 and 9), the sharp pitch-up tendencies associated with the basic wing were delayed by about 0.2 to $0.4C_L$ up to a Mach number of 0.90. However, small destabilizing breaks in the pitching-moment curves usually appeared at lift coefficients only slightly higher than those of the basic wing-fuselage configuration for most of the leading-edge flap combinations investigated (see parts (c) of figs. 6 to 11). For the most part, the leading-edge flap arrangements employed provided no apparent improvements in the pitching-moment curves above a Mach number of 0.90.

The most pronounced aerodynamic effects of the leading-edge flaps investigated were on the drag characteristics. The lift coefficients for minimum drag, as well as the minimum drag generally, were increased by all the leading-edge flap arrangements (see parts (b) of figs. 6 to 11). All the leading-edge flaps investigated reduced the drag in the medium lift range. The 3° and 6° full-span and outboard partial-span flaps (figs. 12 and 13, configurations 2, 3, 6, and 7) usually maintained better maximum lift-drag ratios than any other leading-edge flap arrangement investigated throughout the Mach number range. In general, the improvements due to leading-edge flap deflection were lost at successively lower Mach numbers as the leading-edge flap deflections were increased.

CONCLUSIONS

An investigation of the effects of deflection of a number of leading-edge flap arrangements on the aerodynamic characteristics in pitch of a wing-fuselage configuration with a 45° sweptback wing of aspect ratio 4 indicated the following conclusions:

1. All of the leading-edge flaps investigated reduced the drag in the medium lift range.
2. The 3° and 6° full-span and outboard partial-span flaps gave, for the most part, better maximum lift-drag ratios than any of the other leading-edge flap arrangements investigated throughout the Mach number range.
3. All leading-edge flaps in general increased the lift coefficients for minimum drag as well as the minimum drag throughout the Mach number range investigated.

4. The leading-edge flaps employed usually delayed the sharp pitch-up tendencies of this model by from 0.2 to 0.4 lift coefficient up to a Mach number of 0.90, but provided little improvement at the highest Mach numbers investigated.

5. In general, there were no significantly large effects on the lift characteristics for any of the leading-edge flap arrangements investigated.

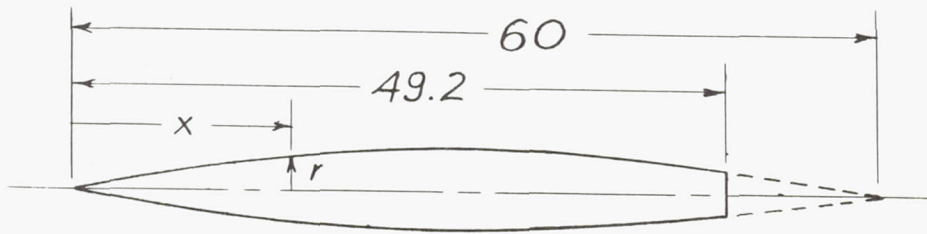
Langley Aeronautical Laboratory,
National Advisory Committee for Aeronautics,
Langley Field, Va., July 2, 1953.

REFERENCES

1. Spreemann, Kenneth P., and Alford, William J., Jr.: Small-Scale Transonic Investigation of the Effects of Full-Span and Partial-Span Leading-Edge Flaps on the Aerodynamic Characteristics of a $50^{\circ} 38'$ Sweptback Wing of Aspect Ratio 2.98. NACA RM L52E12, 1952.
2. Alford, William J., Jr., and Spreemann, Kenneth P.: Small-Scale Transonic Investigation of a 45° Sweptback Wing of Aspect Ratio 4 With Combinations of Nose-Flap Deflections and Wing Twist. NACA RM L52K13, 1953.
3. Spreemann, Kenneth P., and Alford, William J., Jr.: Investigation of the Effects of Leading-Edge Chord-Extensions and Fences in Combination With Leading-Edge Flaps on the Aerodynamic Characteristics at Mach Numbers From 0.40 to 0.93 of a 45° Sweptback Wing of Aspect Ratio 4. NACA RM L53A09a, 1953.
4. Herriot, John G.: Blockage Corrections for Three-Dimensional-Flow Closed-Throat Wind Tunnels, With Consideration of the Effect of Compressibility. NACA Rep. 995, 1950. (Supersedes NACA RM A7B28.)
5. Gillis, Clarence L., Polhamus, Edward C., and Gray, Joseph L., Jr.: Charts for Determining Jet-Boundary Corrections for Complete Models in 7- by 10-Foot Closed Rectangular Wind Tunnels. NACA WR L-123, 1945. (Formerly NACA ARR L5G31.)
6. Osborne, Robert S.: High-Speed Wind-Tunnel Investigation of the Longitudinal Stability and Control Characteristics of a 1/16-Scale Model of the D-558-2 Research Airplane at High Subsonic Mach Numbers and at a Mach Number of 1.2. NACA RM L9C04, 1949.

TABLE I.- FUSELAGE ORDINATES

[Basic fineness ratio, 12; actual fineness ratio 9.8
achieved by cutting off rear portion of body]



Ordinate, in.	
x	r
0	0
.30	.139
.45	.179
.75	.257
1.50	.433
3.00	.723
4.50	.968
6.00	1.183
9.00	1.556
12.00	1.854
15.00	2.079
18.00	2.245
21.00	2.360
24.00	2.438
27.00	2.486
30.00	2.500
33.00	2.478
36.00	2.414
39.00	2.305
42.00	2.137
49.20	1.650

L.E. radius = 0.030 in.



TABLE II.- LIST OF FIGURES PRESENTING DATA

Figure	Configuration	δ_n , deg			Data presented
		A	B	C	
6	1	0	0	0	Basic ↓
	2	3	3	3	
	3	6	6	6	
7	1	0	0	0	Basic ↓
	4	10	10	10	
	5	15	15	15	
8	1	0	0	0	Basic ↓
	6	0	3	3	
	7	0	6	6	
9	1	0	0	0	Basic ↓
	8	0	10	10	
	9	0	15	15	
10	1	0	0	0	Basic ↓
	10	3	6	6	
	11	3	10	10	
	12	3	6	10	
11	1	0	0	0	Basic ↓
	13	3	3	0	
	14	6	6	0	
	15	0	0	6	
12	1	0	0	0	L/D ↓
	2	3	3	3	
	3	6	6	6	
	4	10	10	10	
	5	15	15	15	
13	1	0	0	0	L/D ↓
	6	0	3	3	
	7	0	6	6	
	8	0	10	10	
	9	0	15	15	
14	1	0	0	0	L/D ↓
	10	3	6	6	
	11	3	10	10	
	12	3	6	10	
15	1	0	0	0	L/D ↓
	13	3	3	0	
	14	6	6	0	
	15	0	0	6	



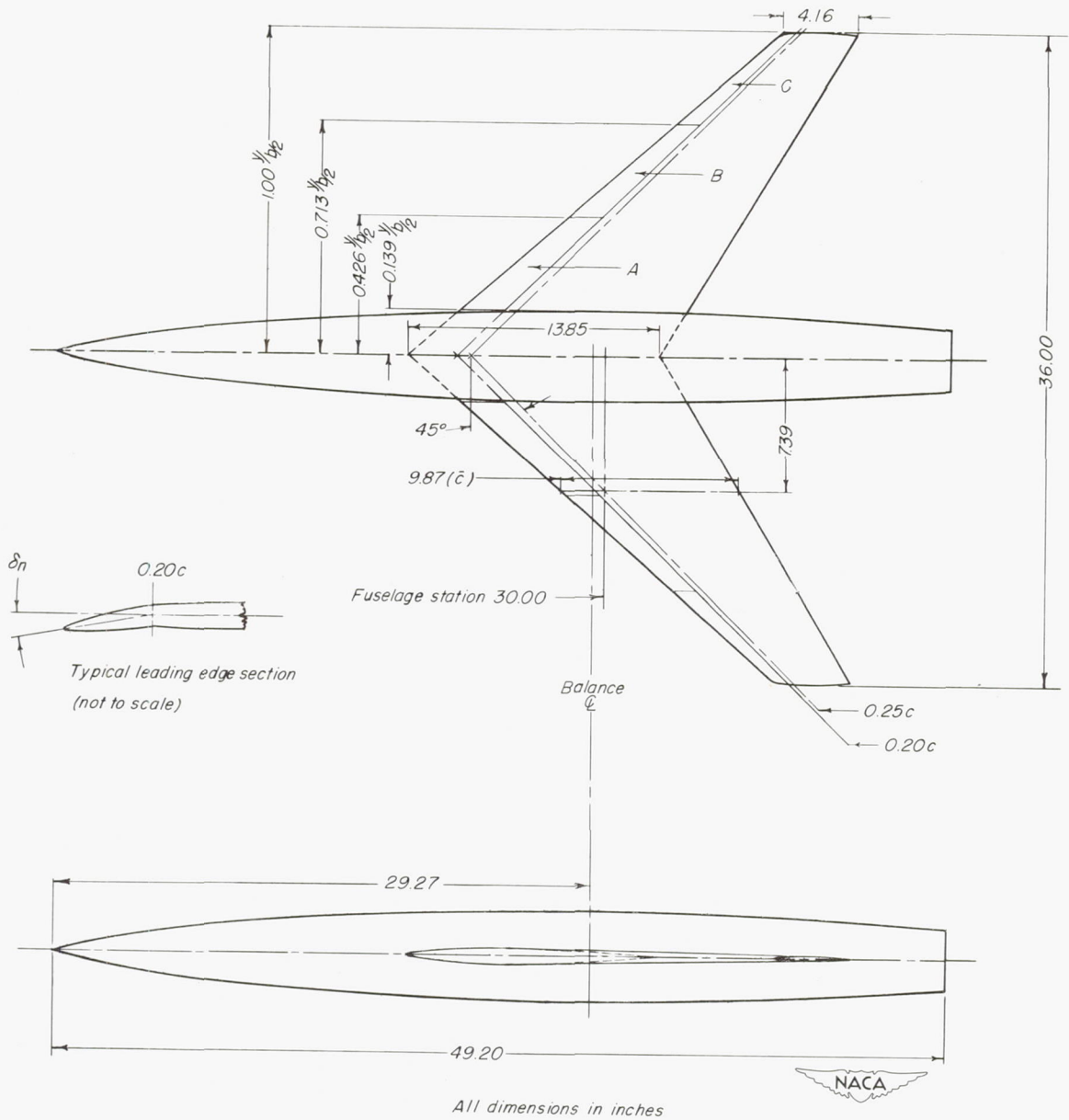
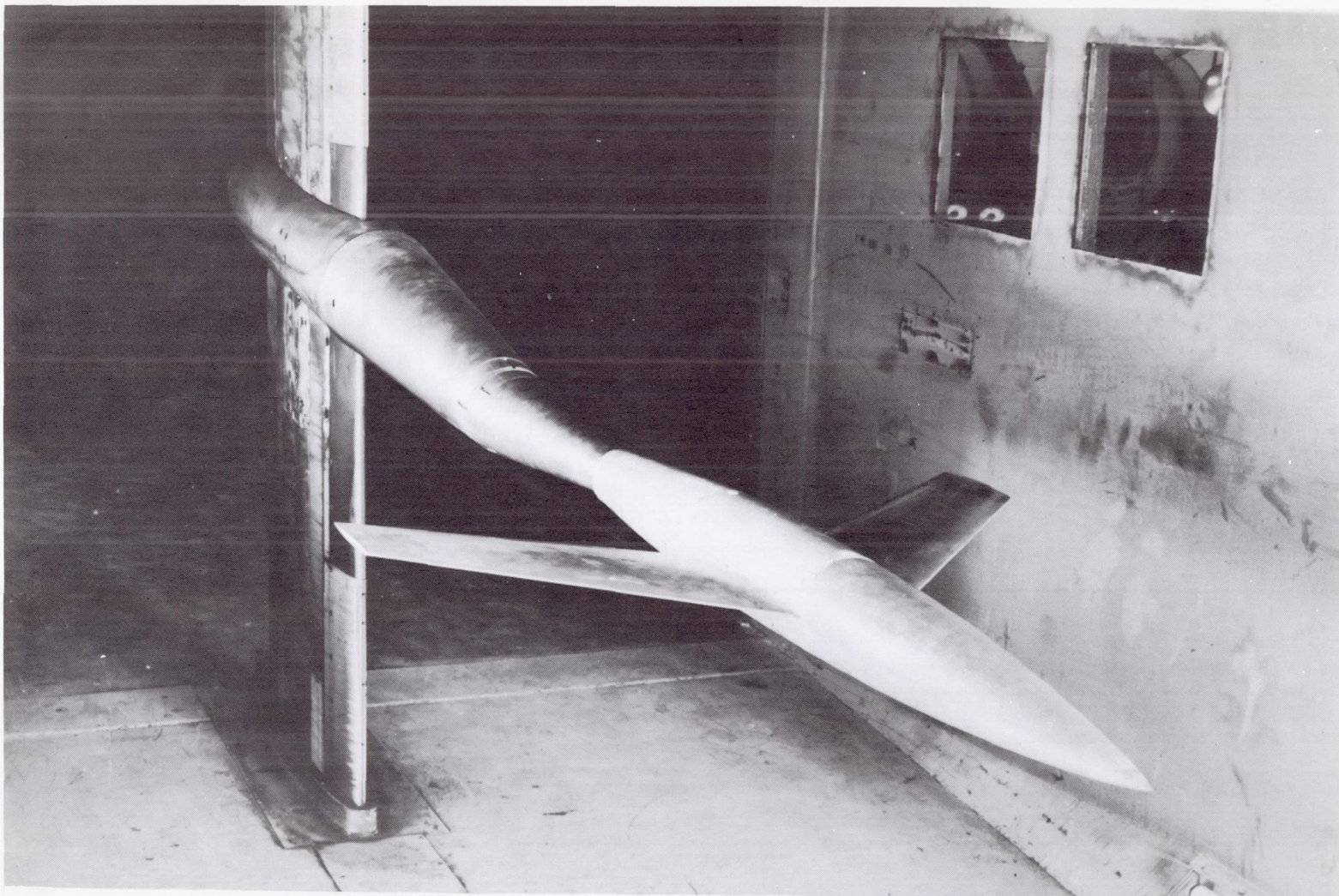


Figure 1.- Test model showing details of the leading-edge flaps.



L-72400

Figure 2.- View of typical test model mounted on sting in Langley high-speed 7- by 10-foot tunnel.

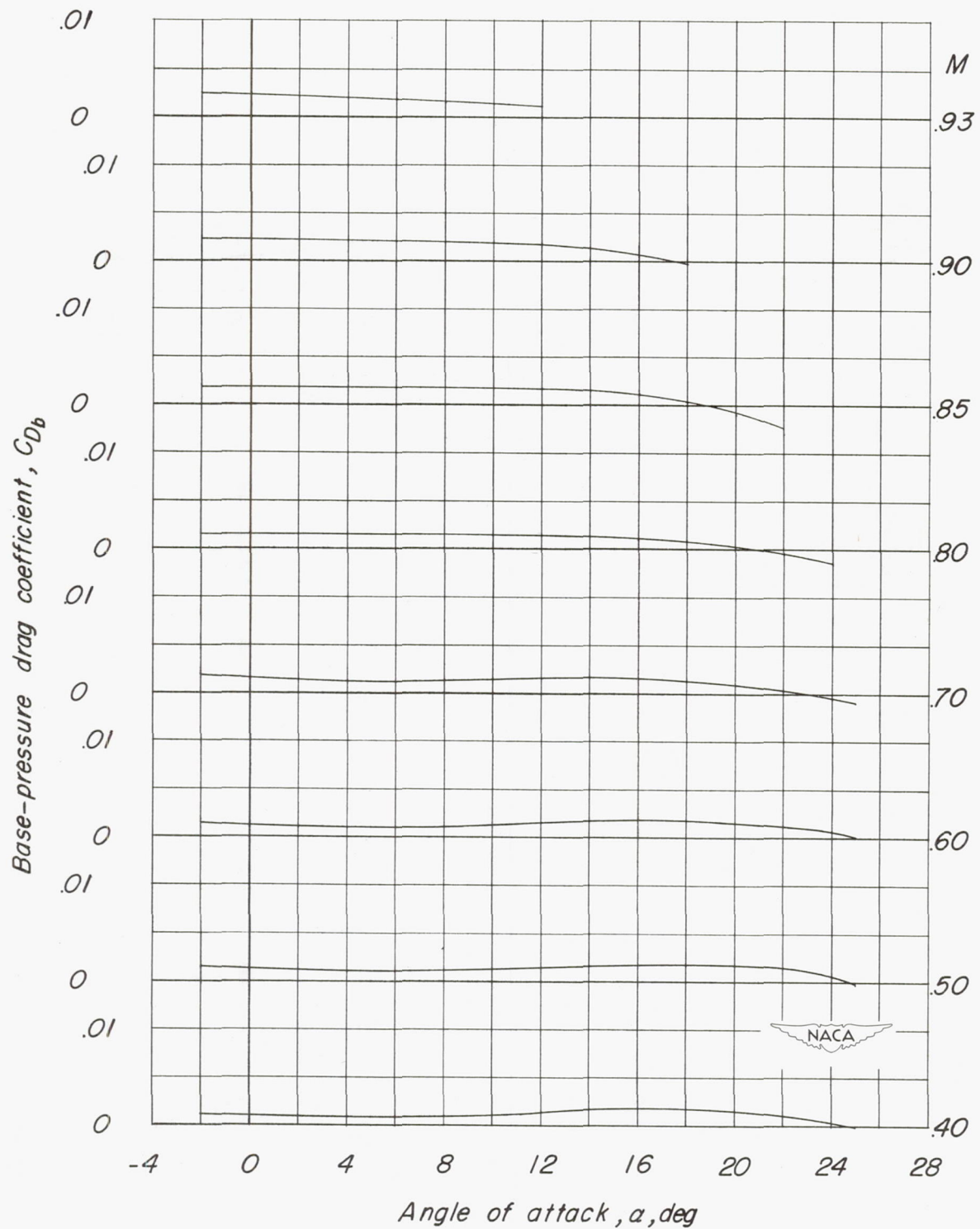


Figure 3.- Variation of base-pressure drag coefficient with angle of attack and test Mach number.

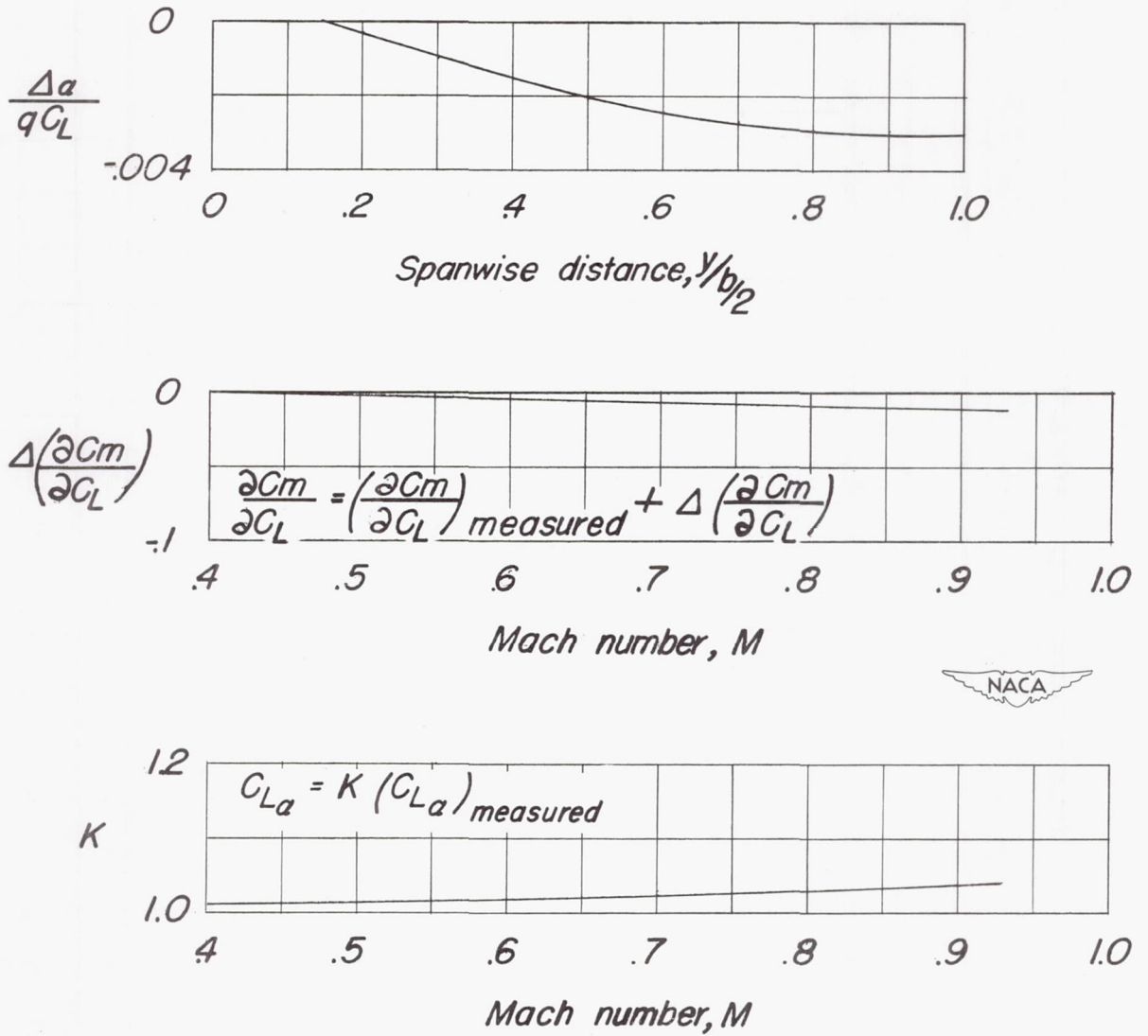


Figure 4.- Correction factors for the effects of aeroelastic distortion.

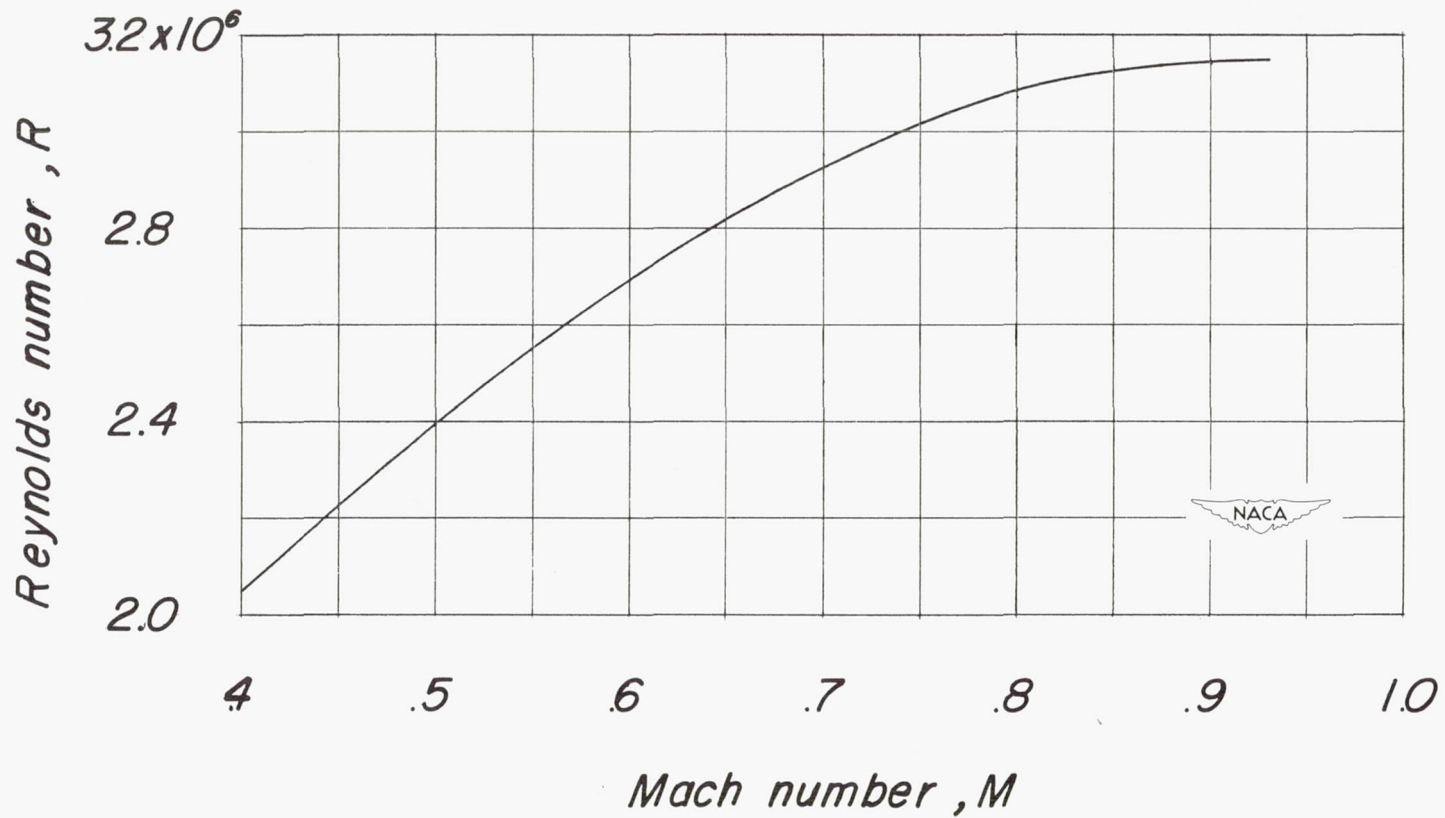
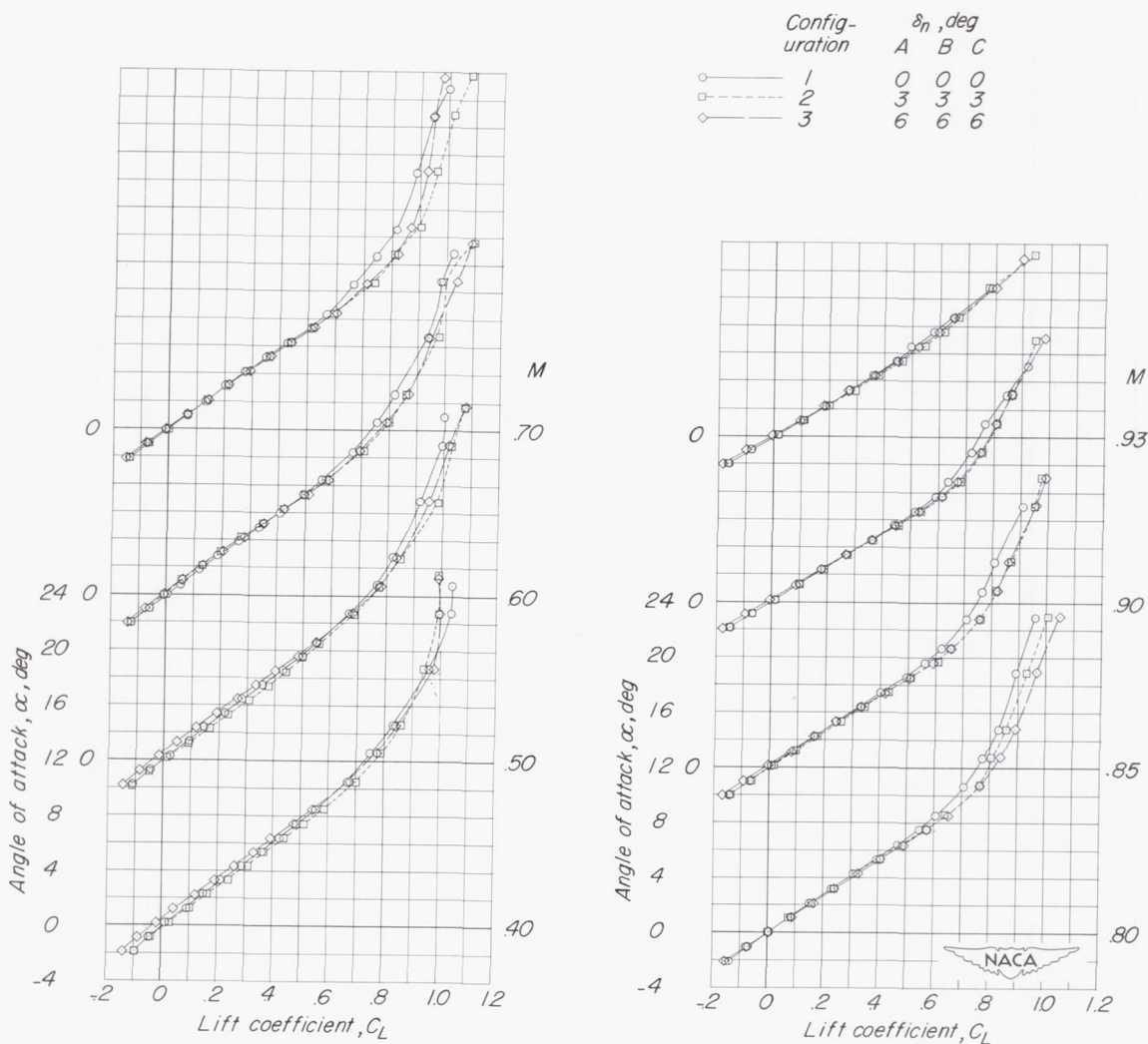
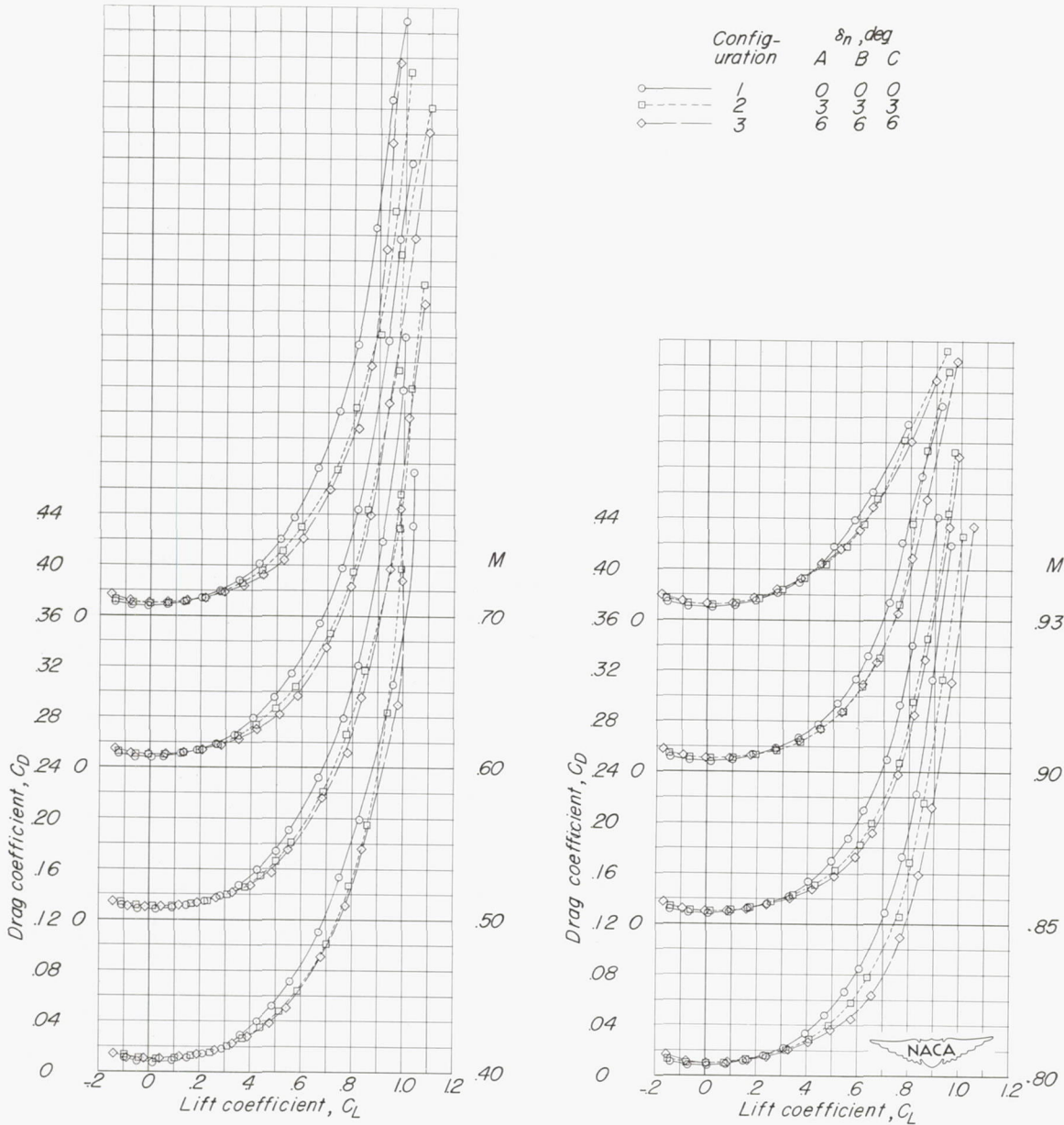


Figure 5.- Variation of mean test Reynolds number with Mach number based on mean aerodynamic chord of wing.



(a) α plotted against C_L .

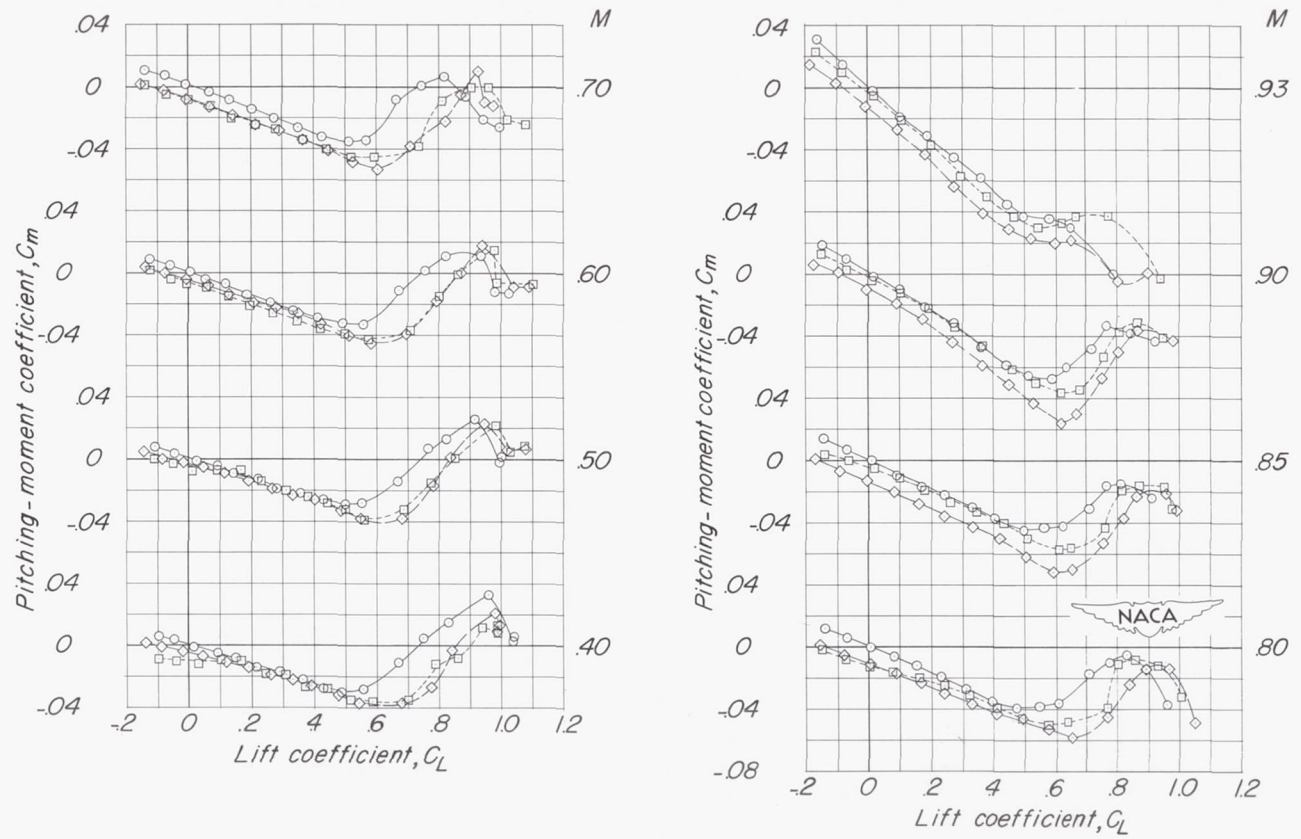
Figure 6.- Aerodynamic characteristics of the wing-fuselage configuration showing the effects of two low-angle full-span leading-edge flaps.



(b) C_D plotted against C_L .

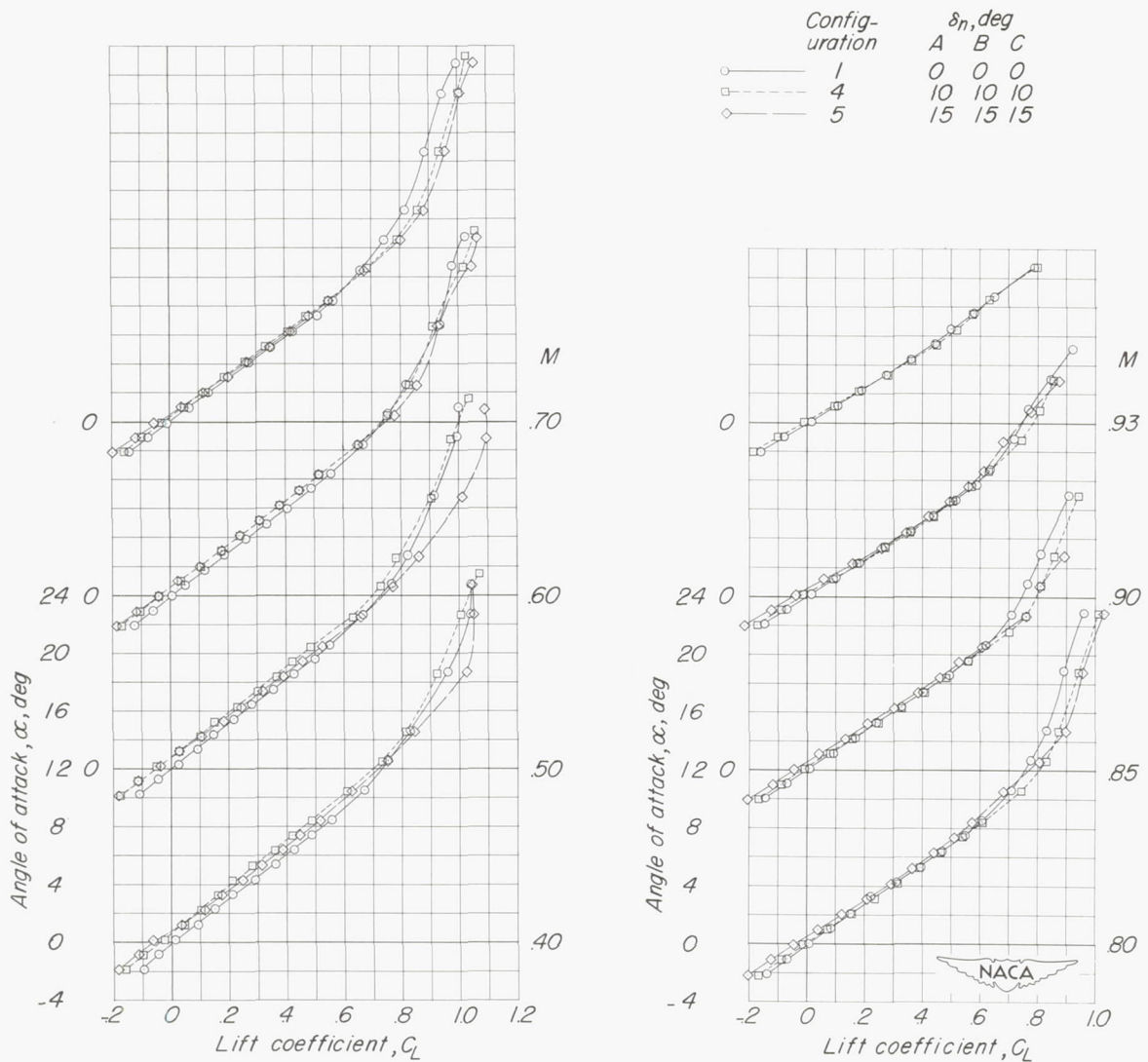
Figure 6.- Continued.

Configuration	δ_n, deg		
	A	B	C
1	0	0	0
2	3	3	3
3	6	6	6



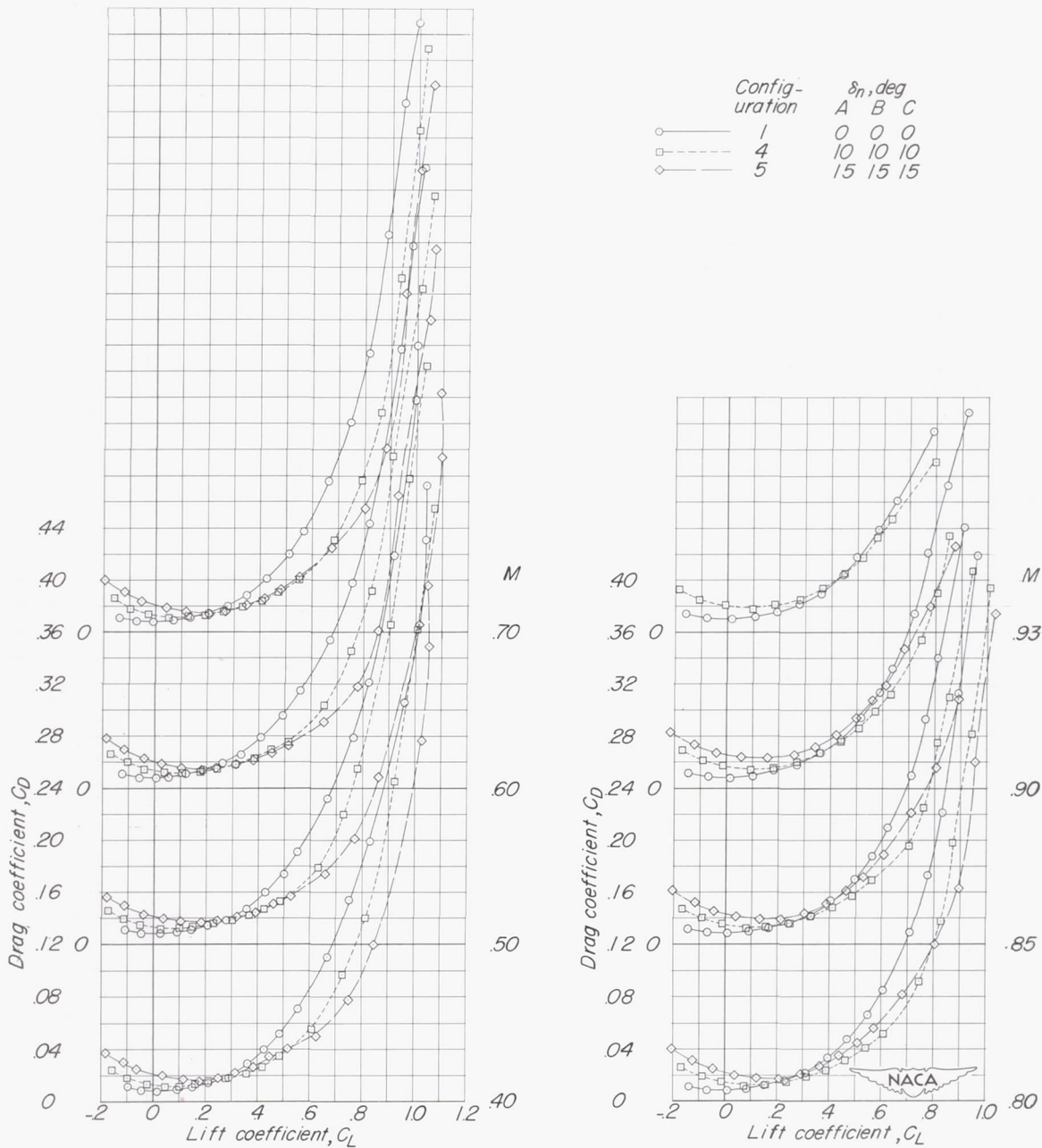
(c) C_m plotted against C_L .

Figure 6.- Concluded.



(a) α plotted against C_L .

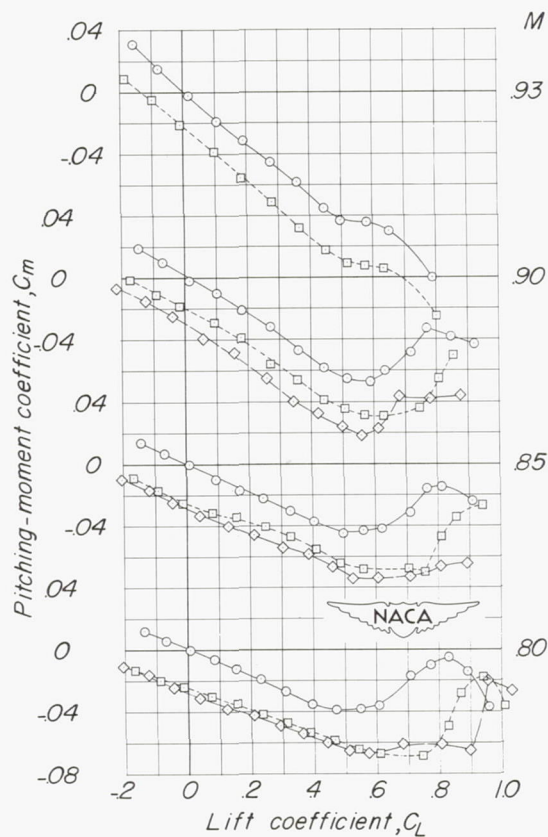
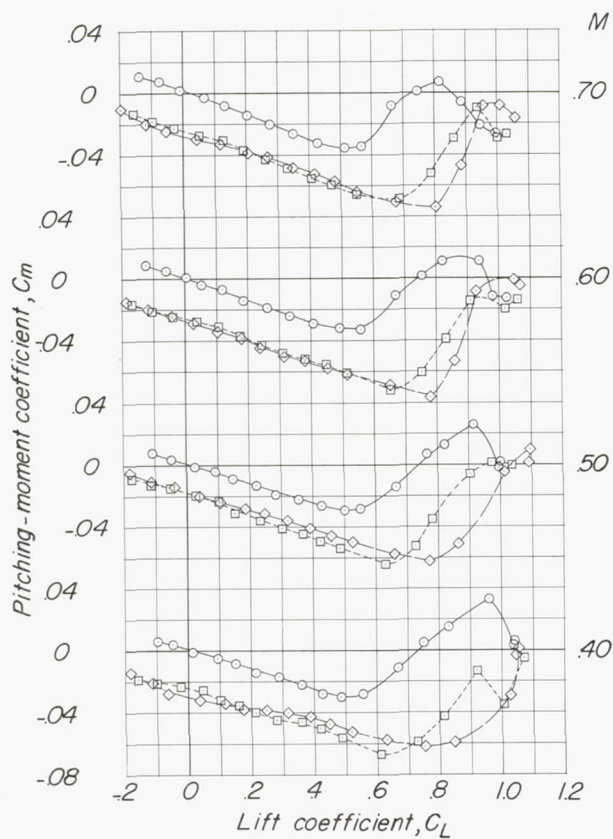
Figure 7.- Aerodynamic characteristics of the wing-fuselage configuration showing the effects of two high-angle full-span leading-edge flaps.



(b) C_D plotted against C_L .

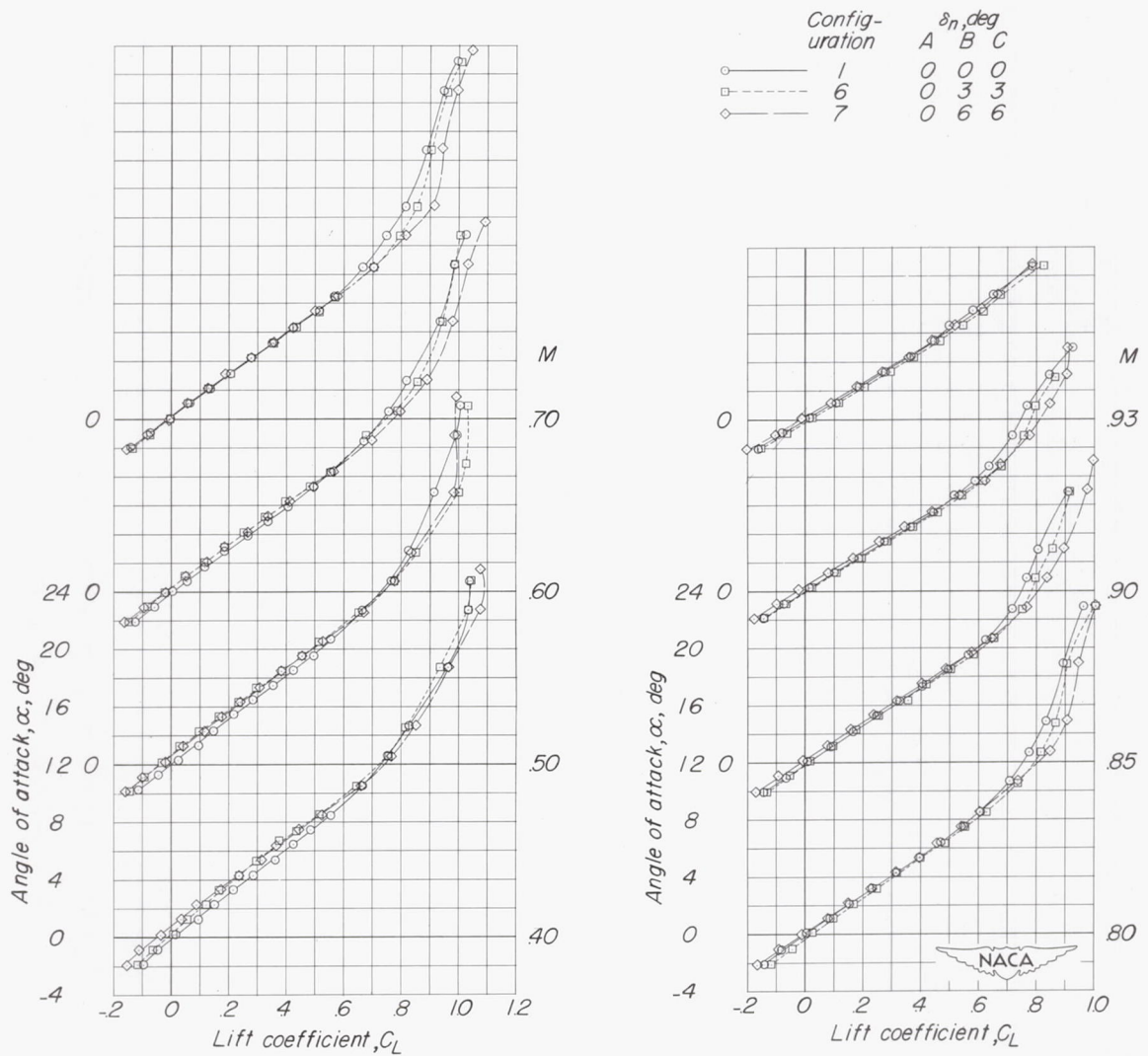
Figure 7.- Continued.

Config- uration	δ_n, deg		
	A	B	C
○ ——— 1	0	0	0
□ - - - 4	10	10	10
◇ ——— 5	15	15	



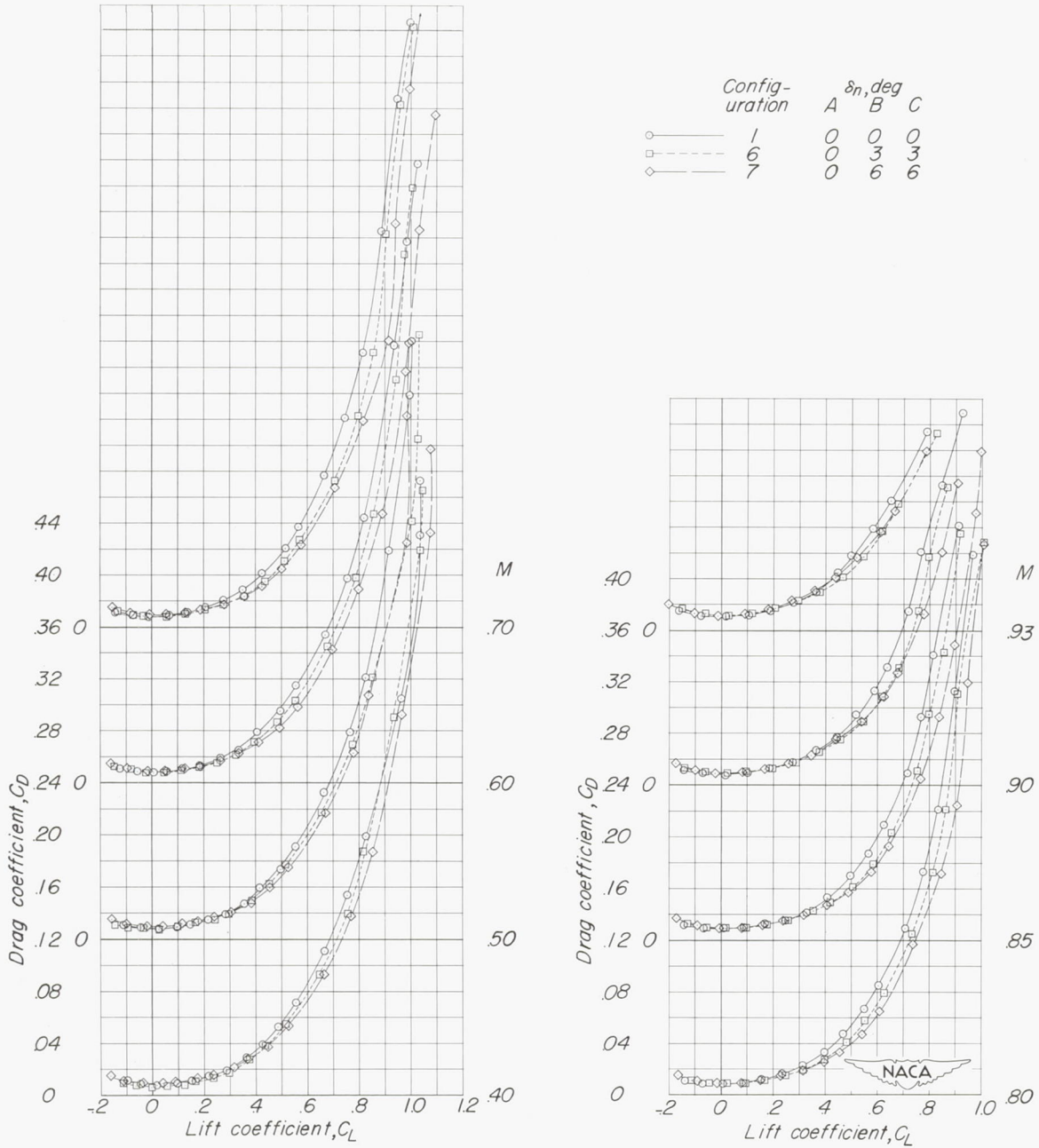
(c) C_m plotted against C_L .

Figure 7.- Concluded.



(a) α plotted against C_L .

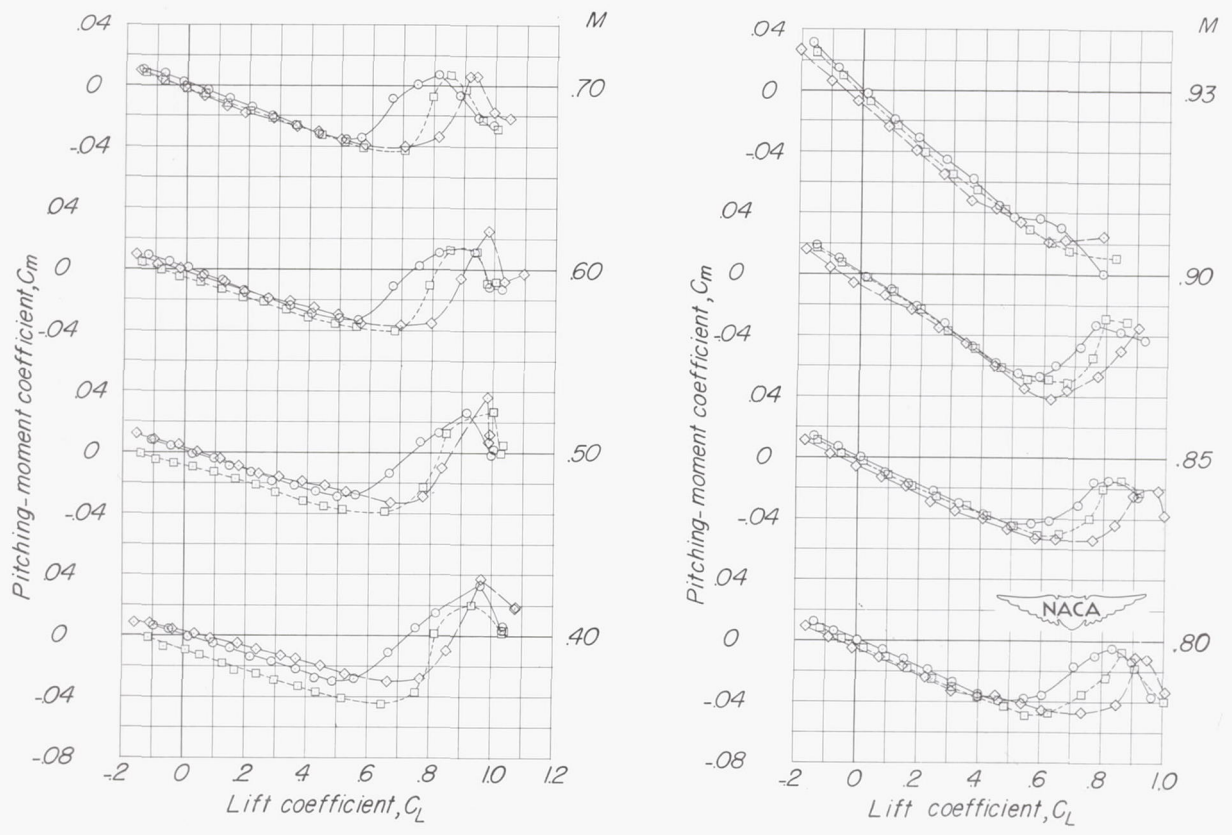
Figure 8.- Aerodynamic characteristics of the wing-fuselage configuration showing the effects of two low-angle outboard partial-span leading-edge flaps.



(b) C_D plotted against C_L .

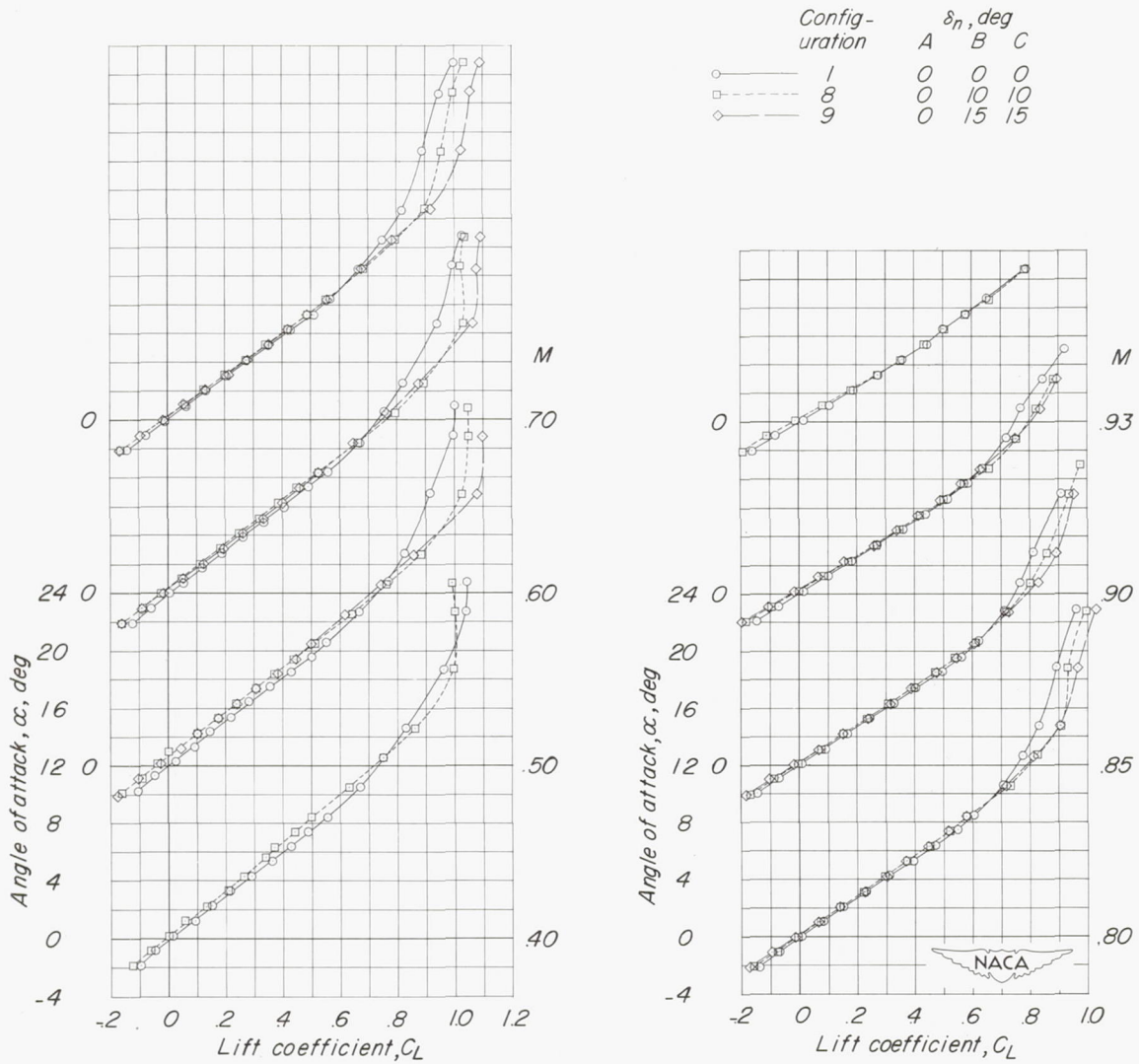
Figure 8.- Continued.

Config- uration	δ_n, deg		
	A	B	C
○ ———	1	0	0
□ - - -	6	0	3
◇ ———	7	0	6



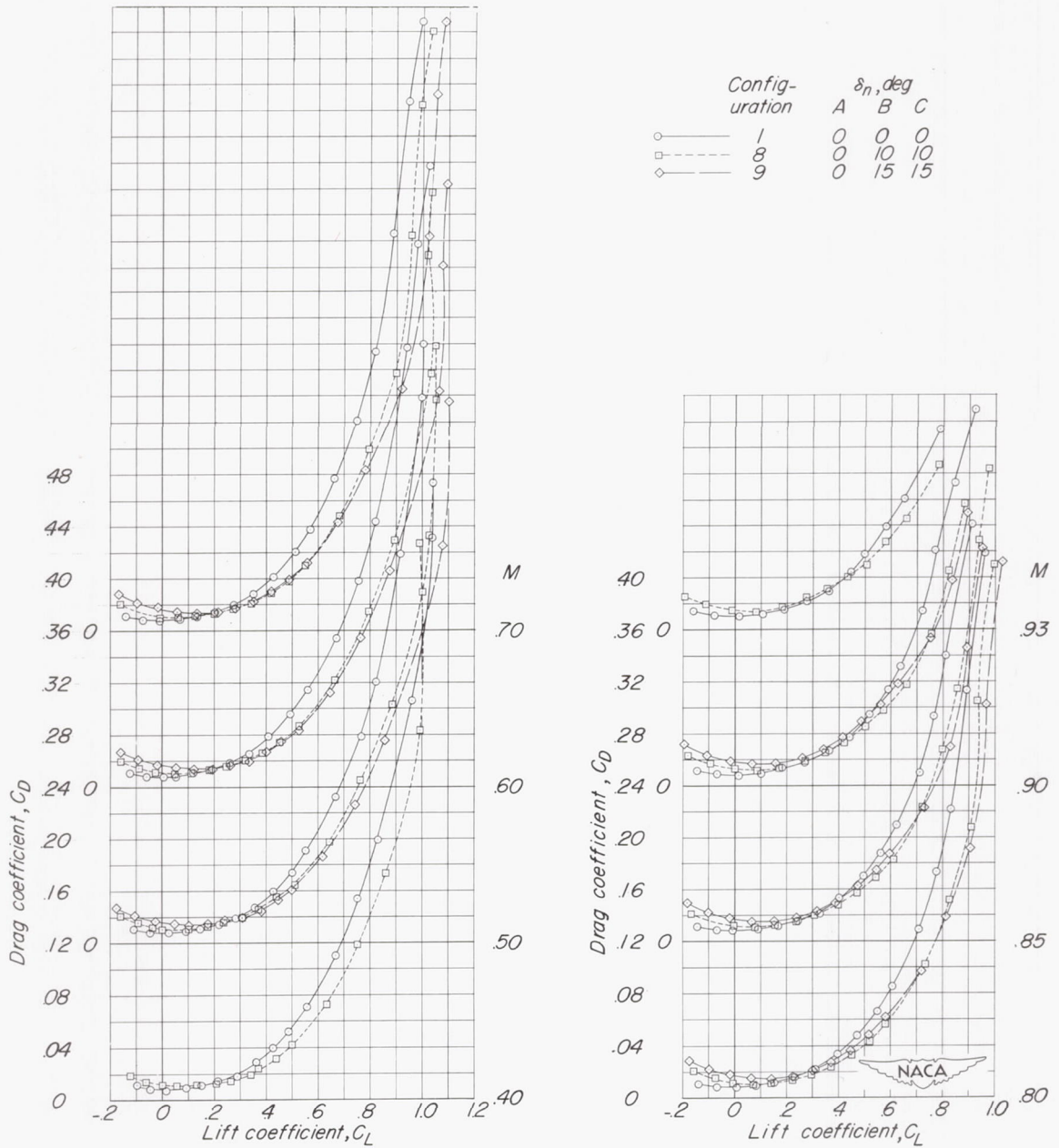
(c) C_m plotted against C_L .

Figure 8.- Concluded.



(a) α plotted against C_L .

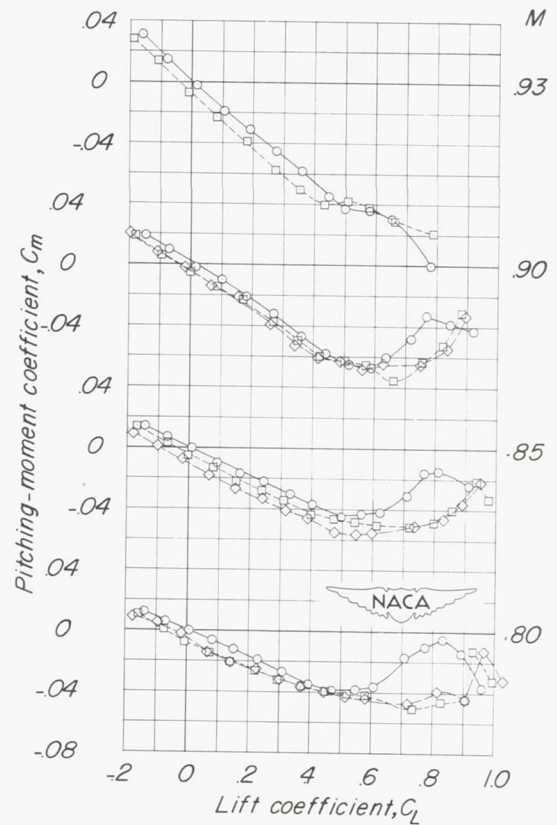
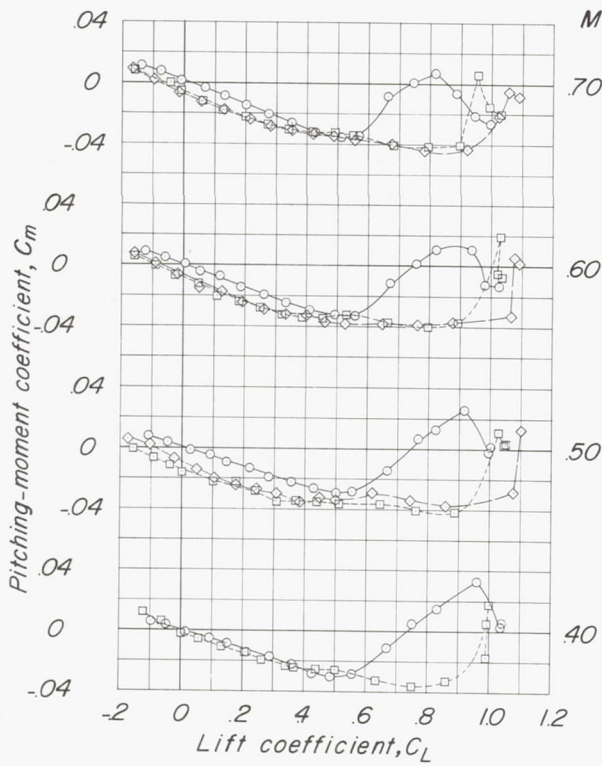
Figure 9.- Aerodynamic characteristics of the wing-fuselage configuration showing the effects of two high-angle outboard partial-span leading-edge flaps.



(b) C_D plotted against C_L .

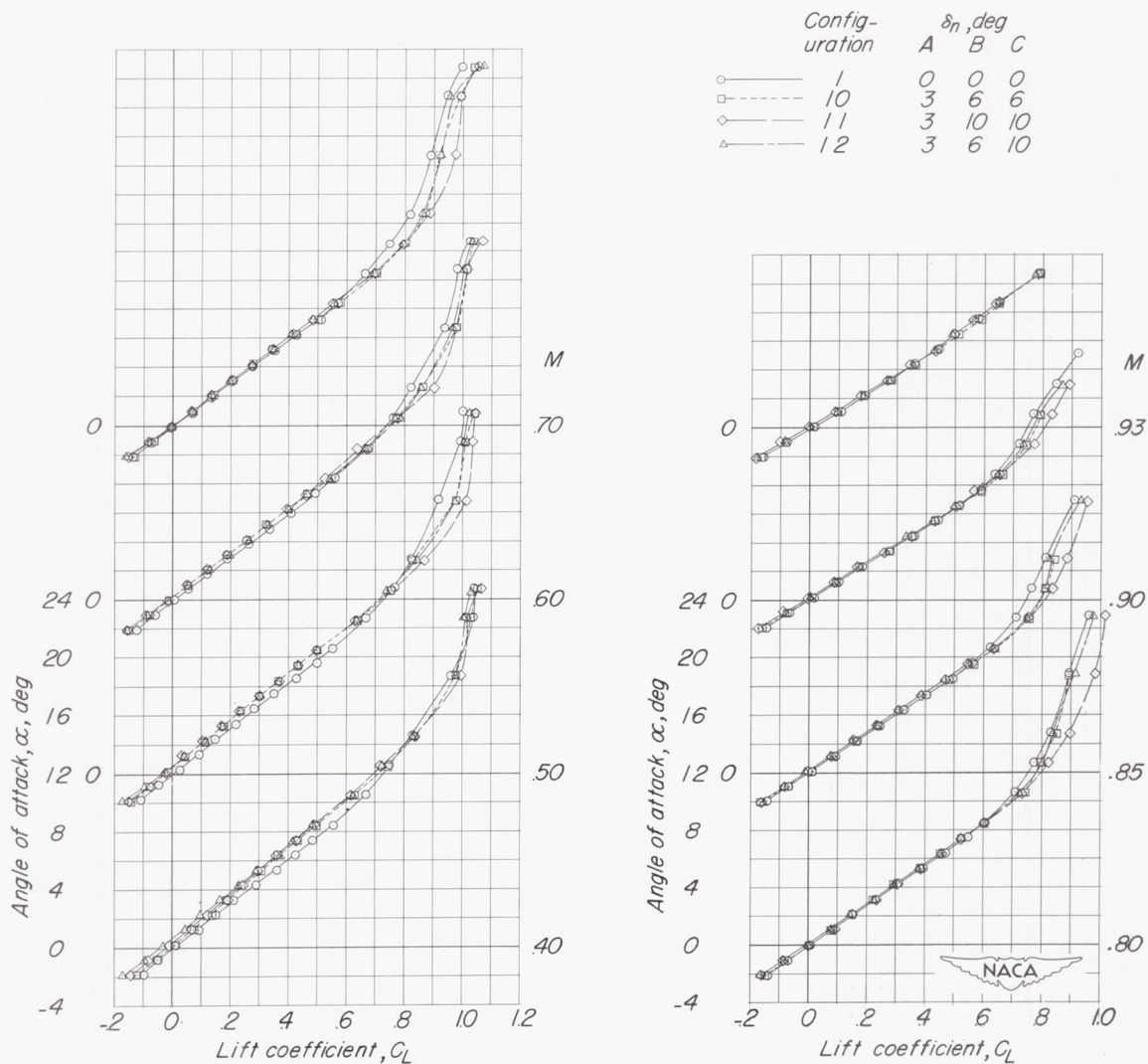
Figure 9.- Continued.

Config- uration	δ_n, deg		
	A	B	C
○ ——— 1	0	0	0
□ - - - 8	0	10	10
◇ ——— 9	0	15	



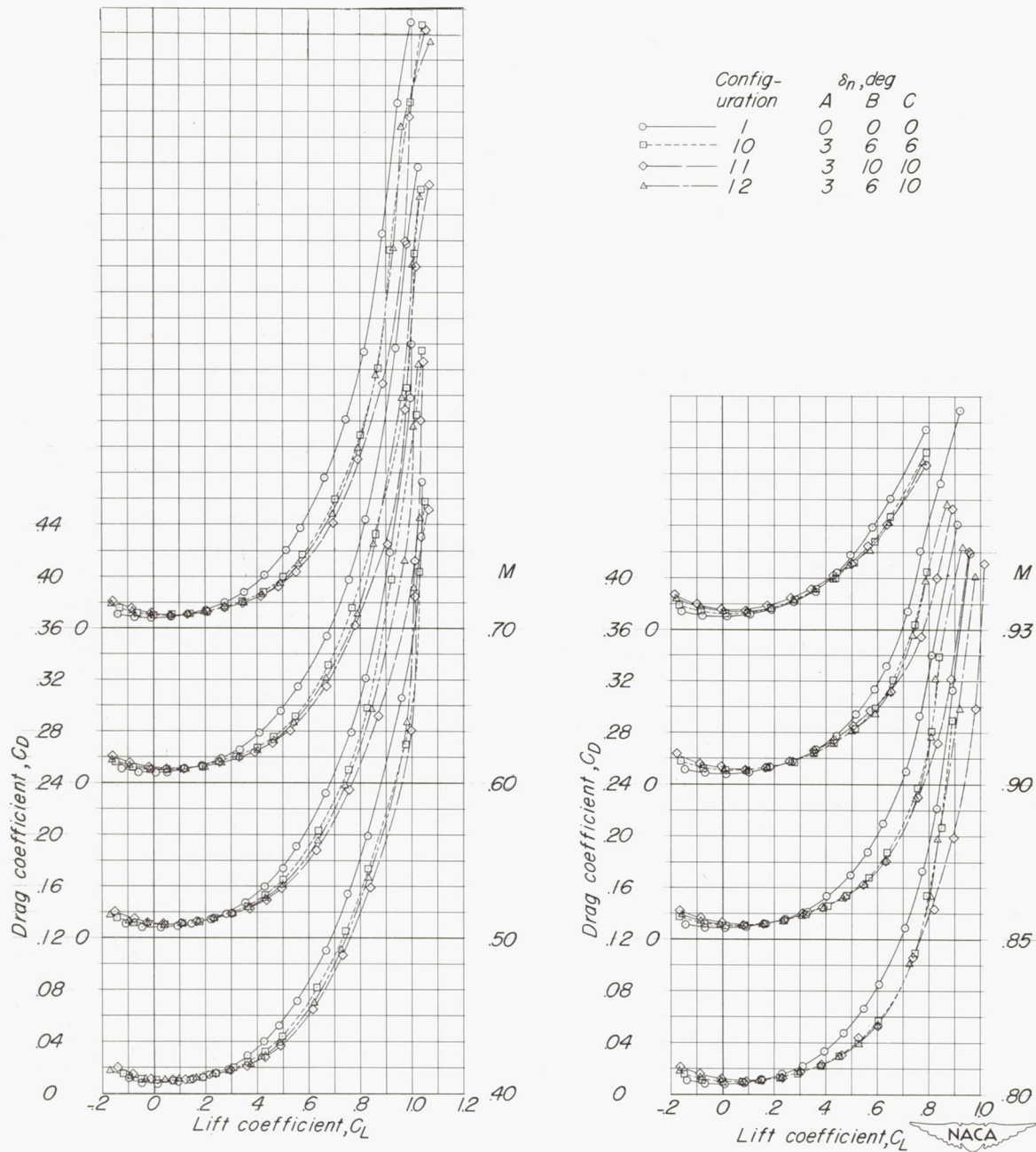
(c) C_m plotted against C_L .

Figure 9.- Concluded.



(a) α plotted against C_L .

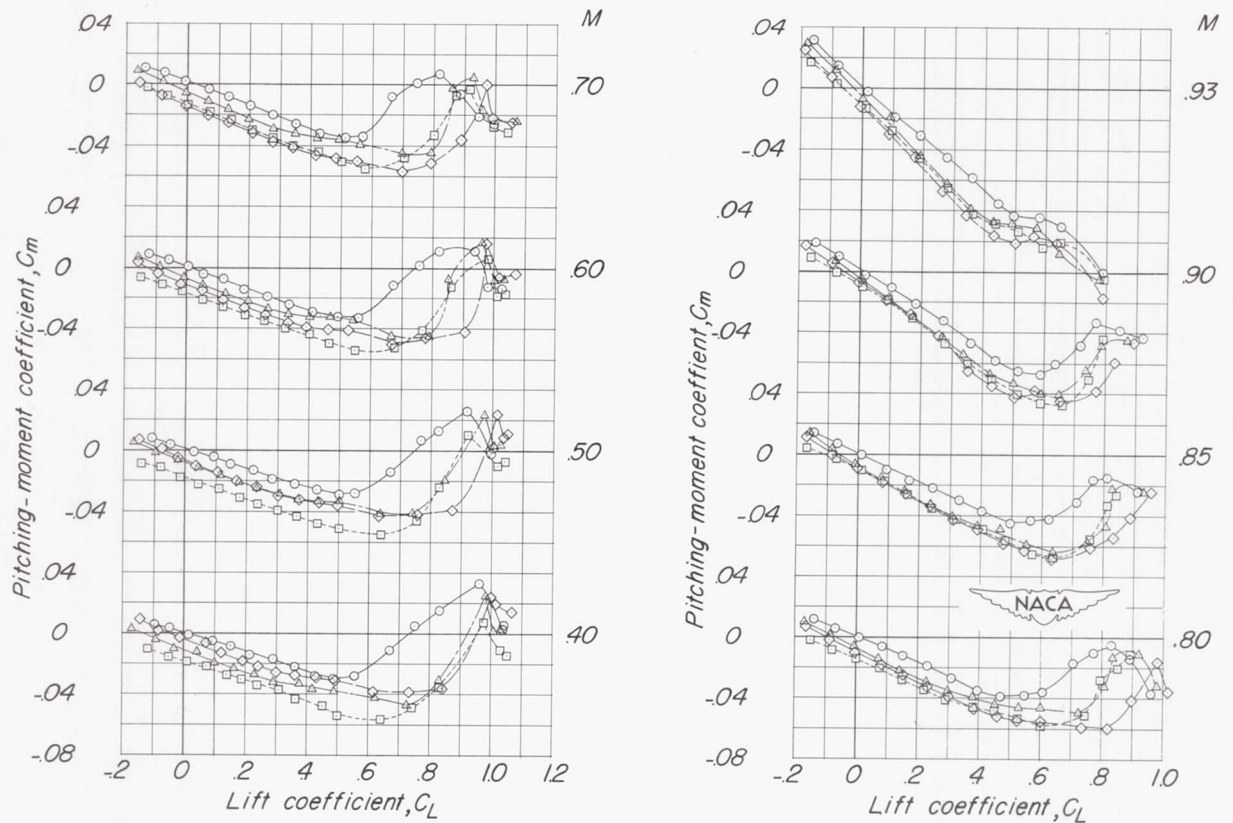
Figure 10.- Aerodynamic characteristics of the wing-fuselage configuration showing the effects of three full-span combinations of leading-edge flaps.



(b) C_D plotted against C_L .

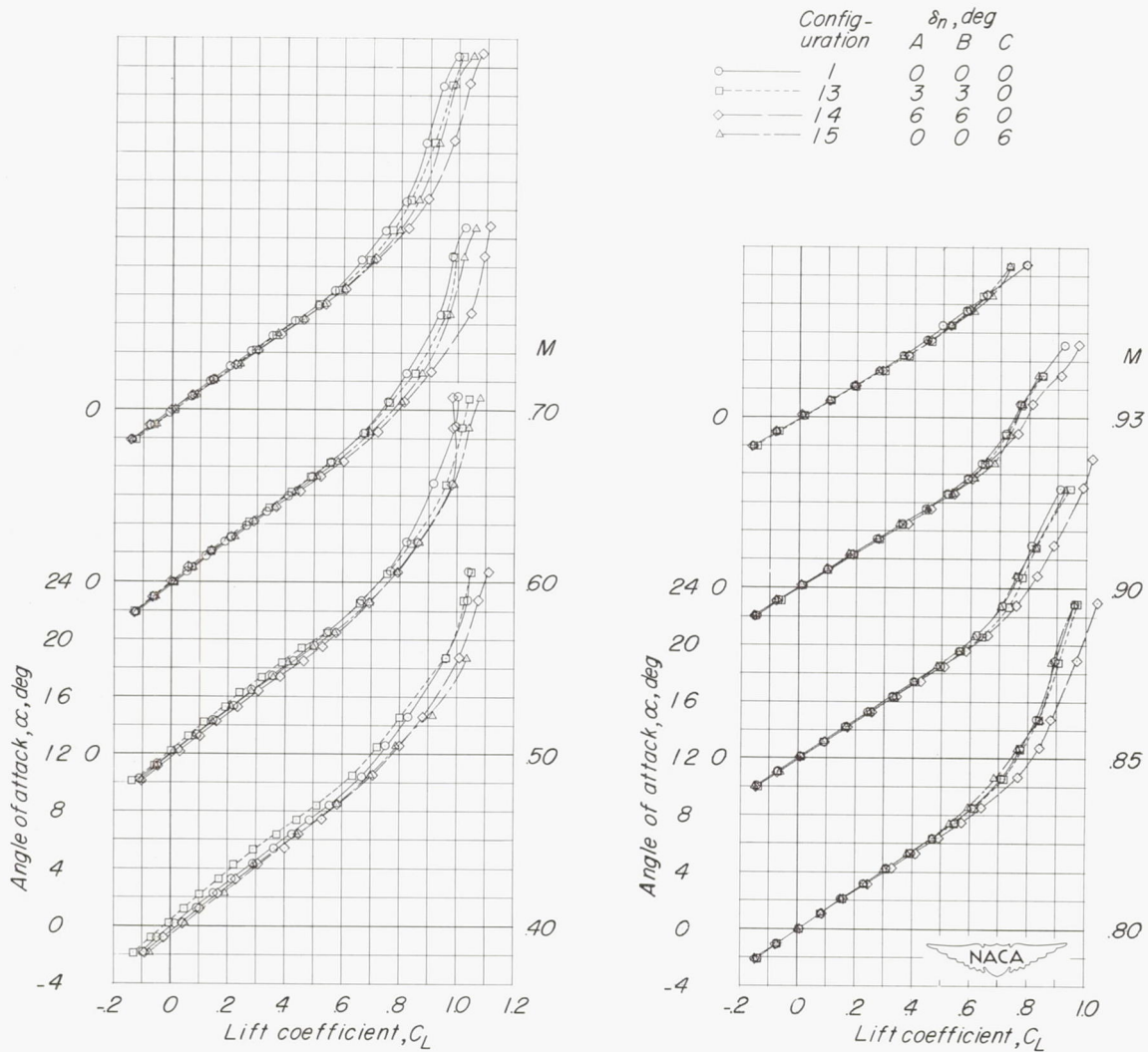
Figure 10.- Continued.

Config- uration	δ_n, deg		
	A	B	C
○ ——— 1	0	0	0
□ - - - 10	3	6	6
◇ - - - 11	3	10	10
△ - - - 12	3	6	10



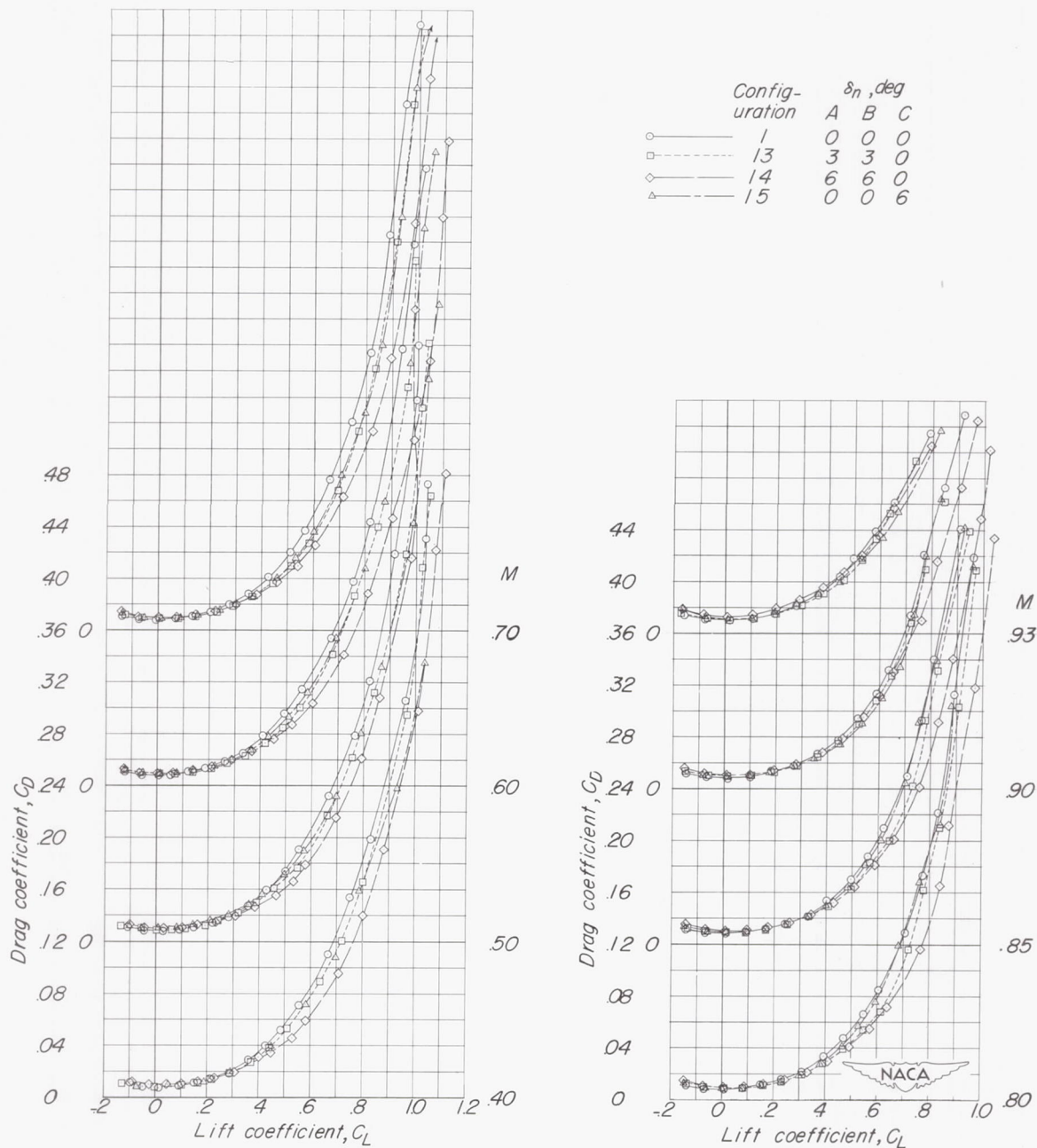
(c) C_m plotted against C_L .

Figure 10.- Concluded.



(a) α plotted against C_L .

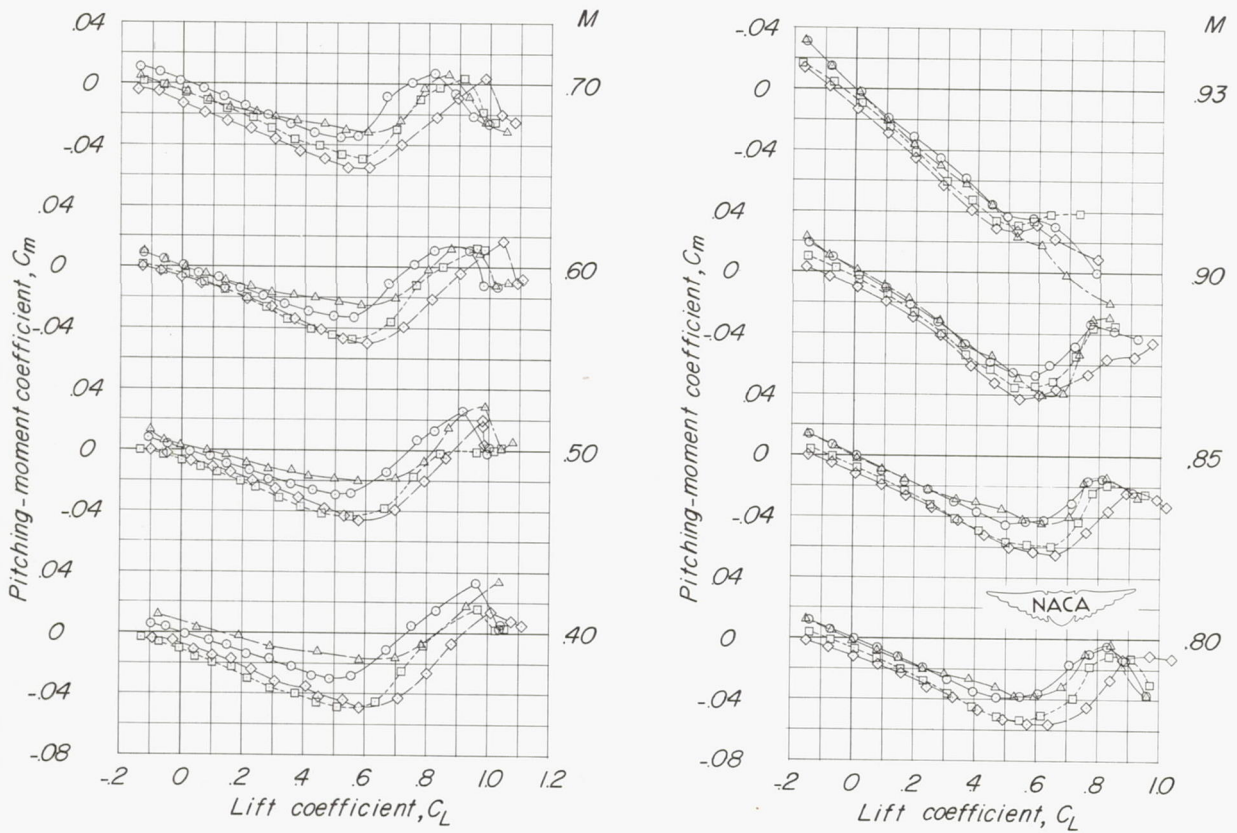
Figure 11.- Aerodynamic characteristics of the wing-fuselage configuration showing the effects of three partial-span combinations of leading-edge flaps.



(b) C_D plotted against C_L .

Figure 11.- Continued.

Config- uration	δ_n, deg		
	A	B	C
○—	0	0	0
□---	3	3	0
◇---	6	6	0
△---	0	0	6



(c) C_m plotted against C_L .

Figure 11.- Concluded.

U

Config- uration	δ_n, deg		
	A	B	C
—	1	0	0
- - -	2	3	3
—	3	6	6
- - -	4	10	10
—	5	15	

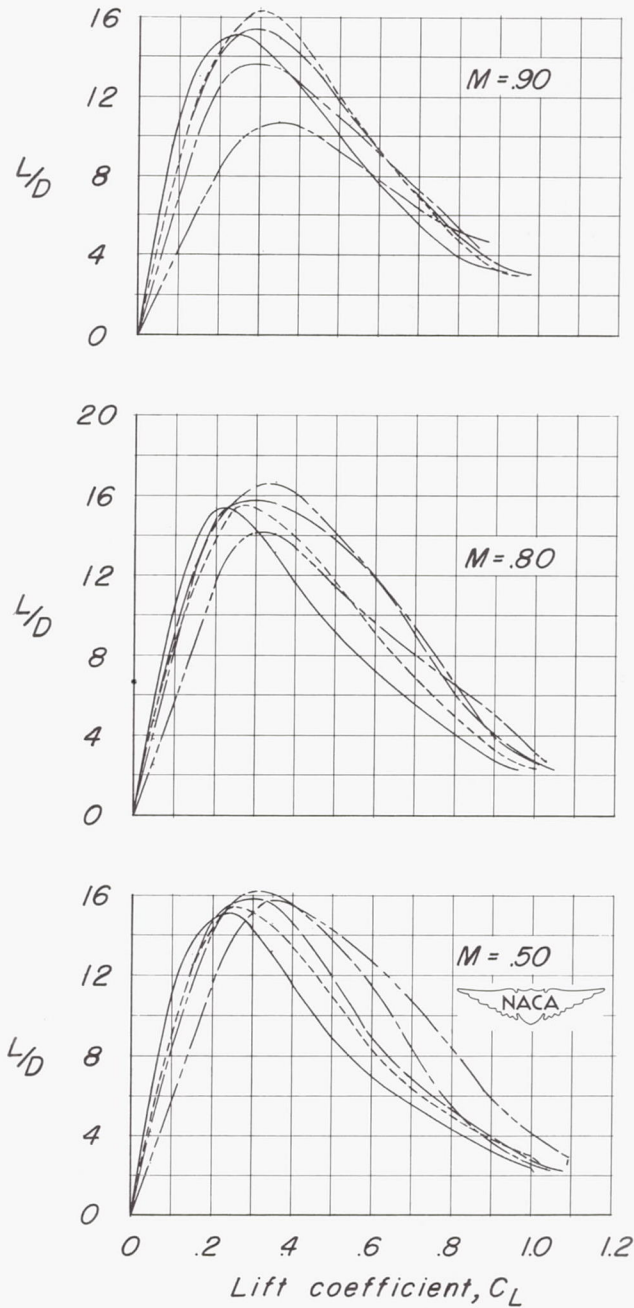


Figure 12.- Lift-drag ratios of the wing-fuselage configuration showing the effects of full-span leading-edge flaps.

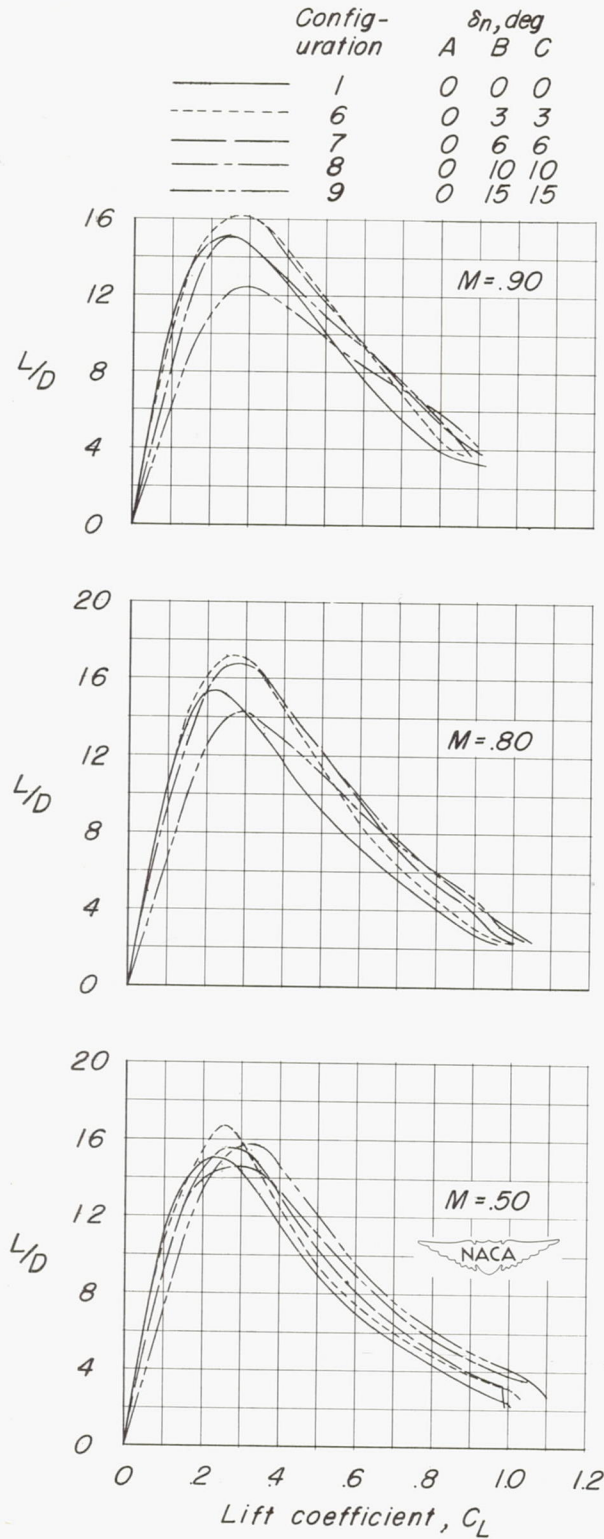


Figure 13.- Lift-drag ratios of the wing-fuselage configuration showing the effects of outboard partial-span leading-edge flaps.

Config- uration	δ_n, deg		
	A	B	C
—	0	0	0
- - -	3	6	6
— · —	3	10	10
- · - -	3	6	10

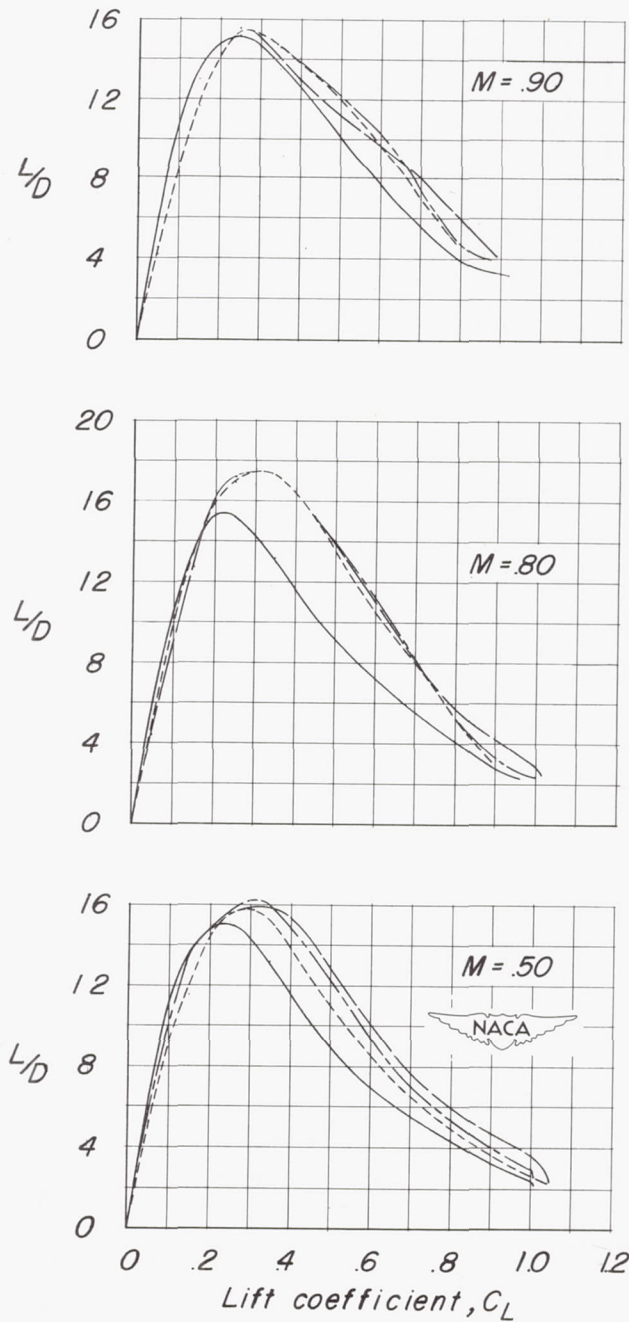


Figure 14.- Lift-drag ratios of the wing-fuselage configuration showing the effects of full-span combinations of leading-edge flaps.

Config- uration	δ_n, deg		
	A	B	C
—	1	0	0
- - -	13	3	3
—	14	6	6
- - -	15	0	0

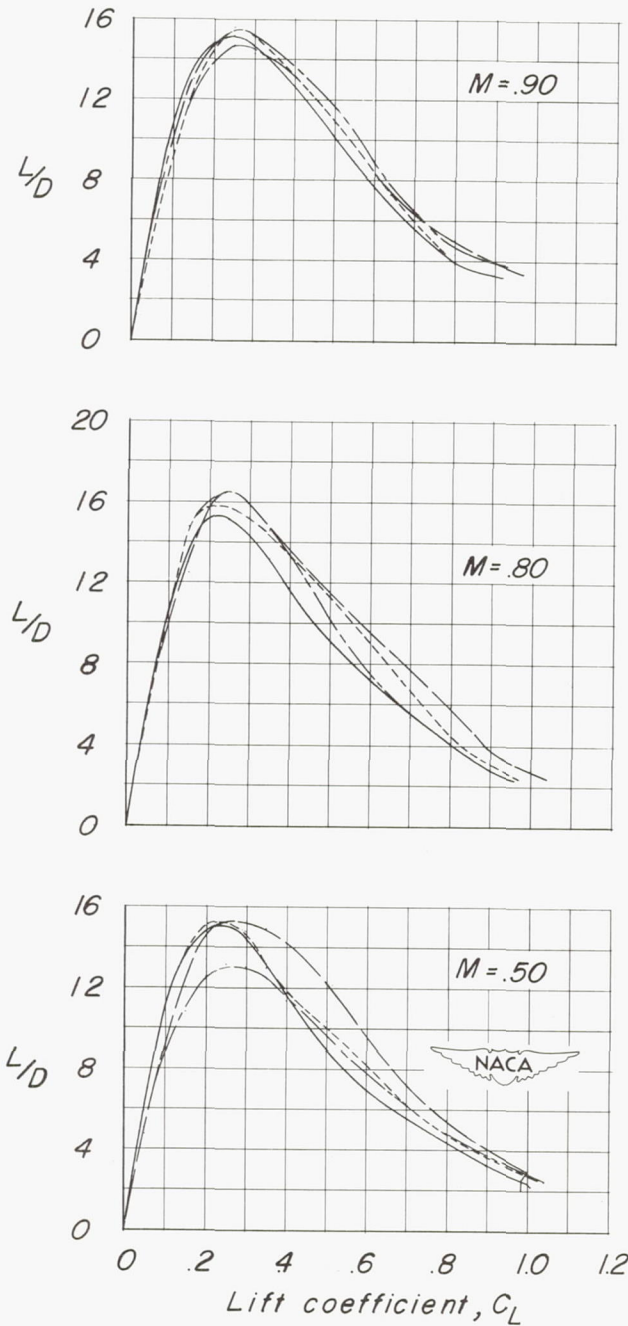


Figure 15.- Lift-drag ratios of the wing-fuselage configuration showing the effects of three partial-span leading-edge flaps.

SECURITY INFORMATION

CONFIDENTIAL

CONFIDENTIAL